Simulator Validation and Evaluation Part II

Presented By

David R. Gingras
Vice President
Bihrle Applied Research Inc.
Hampton, VA

SIMULATOR VALIDATION AND EVALUATION PART II: CONTENTS

EXAMPLES OF FLIGHT MODEL VALIDATION AND EVALUATION

The follow sections contain three case studies demonstrating some of the key issues surrounding the development of aerodynamics models for use in flight simulation. The first project described below was an engineering simulation model development effort in direct support of a military trainer configuration development and flight support. In this case the simulation was modified with wind-tunnel data then validated. The simulation was then used to explore new flight characteristics and help determine aircraft modifications. Once modifications were made to the aircraft, the airplane was flight tested to validate the prediction made with the simulation. The second example provided is a validation and update effort to improve the fidelity of the US Navy's F/A-18CD engineering High-Lift Aerodynamics model. The F/A-18 validation effort demonstrates a novel approach to simulation model validation using flight data. The last case study presented here is an AV-8B trainer model development and validation effort, where reduced flying-qualities and performance data, flight data, and pilot opinion were used to update and validate an aerodynamics model.

Before presenting the case studies, a review of terminology in the context in which it is to be used in the studies provided below.

Case Study Terminology

Model Development

Model development is the process of improving an existing model to increase functionality.

Model Functionality

Model Functionality, as used in this presentation, is the ability of a model to account for the physical and operational state of the object being modeled. For example, increased aerodynamics model functionality can be the addition of data to allow the modeling of independent control surfaces. Another example may be the introduction of data to expand the angle-of-attack range for which the model is valid.

Model Verification and Validation

The terms verification and validation are often misused which can lead to confusion. Below are the respective formal definitions of each word.

Verification – Process of proving to be true by evidence; confirm[1]

Validation – Process of basing on evidence or sound reasoning

The key words that differentiate the two meanings are "proving" and "confirm" rather than "basing." Comparisons to verify models should result in NO appreciable error. Comparisons to validate usually contain a certain level of acceptable error.

A good example of a verification effort is the process of confirming the functionality and output of a simulation model has not changed after a rehost to another computer or language. An example of a validation is the comparison of climb performance test results in a simulation with flight data.

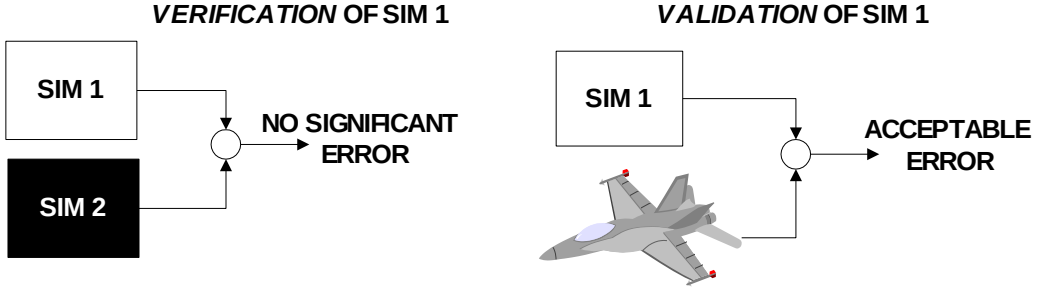

Figure 1. Definition of verification and validation.

Direct Simulation Overdrive (DSO)

Direct simulation overdrive is a technique that may be used during simulation validation and verification and involves replacing simulation variables at each time step during a simulation run to compute a new simulation state. The data used to replace simulation variables may come from another simulation, flight data, or some other analytical means. The objective for using DSO is to minimize propagated errors during verification and validation tasks. By overdriving a simulation variable that is state based, small modeling errors will not adversely affect simulation comparisons. During direct simulation overdrive, the aircraft state is computed by the simulation at each time step. An example application of this technique is the DSO of control surface deflections from a flight test maneuver. As seen in the diagram below (Figure 2), flight test-recovered histories of surface deflections are used to replace simulation computed surface deflections. This ensures that the remainder of the simulation uses identical deflections to those used in flight. The output of the simulation then reflects the integrated simulation response to measured control surface deflections.

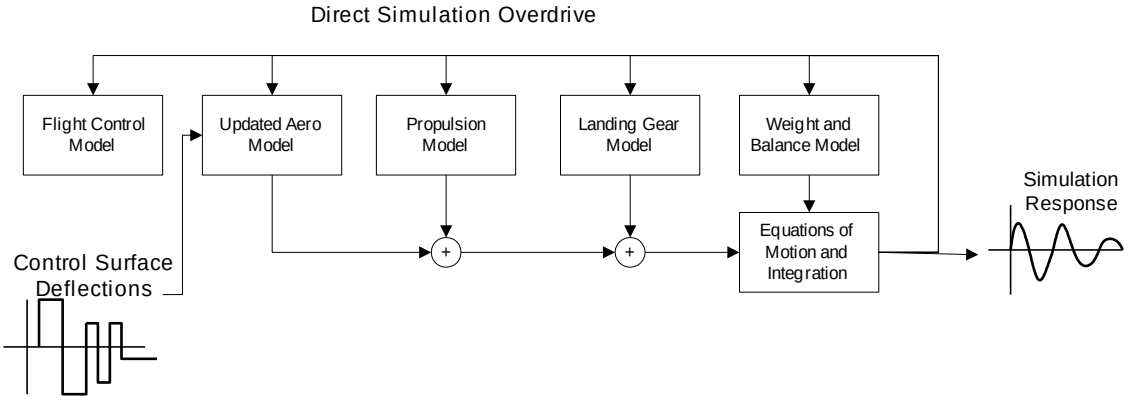

Figure 2. Diagram illustrating direct simulation overdrive.

Model Isolation Overdrive (MIO)

Model isolation overdrive is similar to direct simulation, but typically more simulation variables are overdriven and the simulation state is NOT computed at each time step. During MIO simulation runs, all required input to a model must available for overdrive, such as body axis rates, attitude angles, surface deflections etc. The MIO technique allows the verification and validation engineer to isolate a particular simulation model during a simulation run. This is a valuable capability to have during validation and verification efforts since it allows the engineer to compare the simulation force and moment output directly

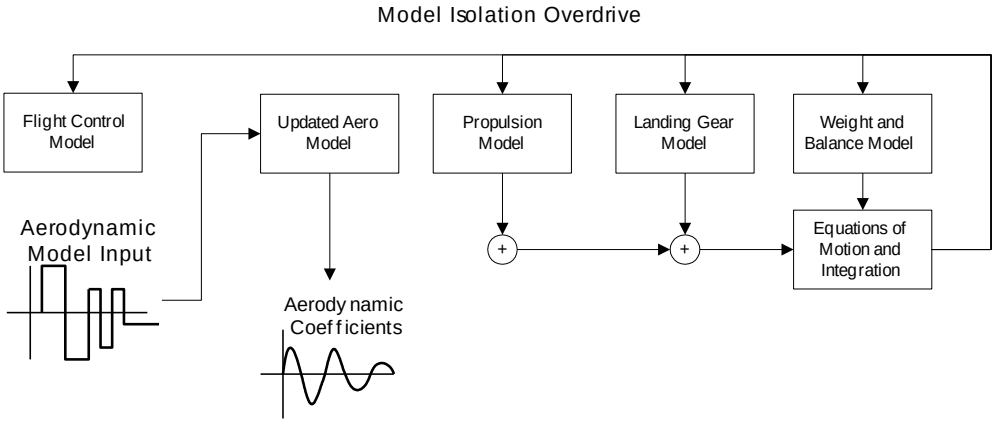

Figure 3. Diagram illustrating model isolation overdrive.

with flight test extracted results with no propagation errors though integration. An MIO example is provide in the diagram below, Figure 3.

In this example the aerodynamics model is isolated. All inputs to the aerodynamics model are overdriven, The output from the model represents the aerodynamics model's response to the measured input. The output of MIO runs is not simulation-state time dependent, unless there is an internal simulation state being computed by the isolated model.

Direct Coefficient Comparison (DCC)

Direct coefficient comparison, as presented in the case studies, is the process of comparing the output of a MIO in coefficient form with coefficients extracted from flight data.

Data Consistency and Compatibility

In the case studies below you will read the terms data consistency or data compatibility. The terms refer to validation data quality. Data quality is vitally important in all simulation model development validation efforts regardless of the techniques used. The cliché of "garbage in = garbage out" truly applies in the world of simulation development and validation.

Data consistency is the ability to verify data with data from another source. For example, redundant measured flight-test parameters can be used for data consistency checks. Such a check might involve reconstructing sensor locations from measured data and comparing them to known location. Often, data consistency checks result in further calibration of measured data.

Data compatibility is the ability to use data with other sources of data. This ensures "apple to apple" comparison. The task of checking and ensuring data compatibility can be a simple as checking the units of two signals to be compared or combined some how, or a complicated as performing several axes transformations to ensure forces you are measuring are in the same coordinate system.

System Identification (System ID)/Parameter Identification (PID)

System Identification involves the identification of a mathematical model form that represents a given dynamical system. Parameter identification is the art and science of identifying physical characteristics of an object from the dynamics response of that object to a prescribed input. In typical modeling efforts, system ID is used as a first step to determine model dependency and functionality. Regression techniques are often used here. Once a suitable model has been postulated or identified, PID can be used to identify model parameters. Both processes involve the minimization of a cost function by estimating parameters in a given set of equations. Several methods/techniques exist for performing System ID and PID. The main issue that accounts for differences in techniques are the assumptions used for the criterion used to optimize the estimates. The assumptions are dependent on the existence of external disturbances such as gusts or vibration and measurement noise in the data. Techniques can be categorized in one of three main groups, Equation Error, Output Error, and advanced Statistical Techniques, which include Maximum Likelihood and Kalman Filtering Techniques. The following paragraphs provide a brief overview of equation error methods and output error methods. Since the case studies to be provided did not make use of the advanced statistical techniques, only minor mention of them is made here. A more detailed discussion may be found in the references provided at the end of this section.

Equation Error techniques are based on the principal of least squares. The technique is commonly used in curve fitting and regression analysis. The method minimizes the "equation error" which can be defined as the difference between the computed model output and true output. The result is model representing measured data with a smooth curve. Equation error estimates are solved directly, but can be biased by measurement error in the truth data. Estimate variance is affected directly by measurement noise and process noise.

Figure 4 contains an example of the computation flow to estimate aerodynamics force derivative using the equation error technique. Control deflection data and state information from a maneuver are used with the measured output from the flight in the least squared solution to compute the coefficients.

Output Error techniques minimize the errors of between the model output and actual output of the system using the same input. The method assumes that no gusts or turbulence are present and only the measured output contains noise. Output error estimates require a nonlinear optimization, which in turn requires an iterative solution.

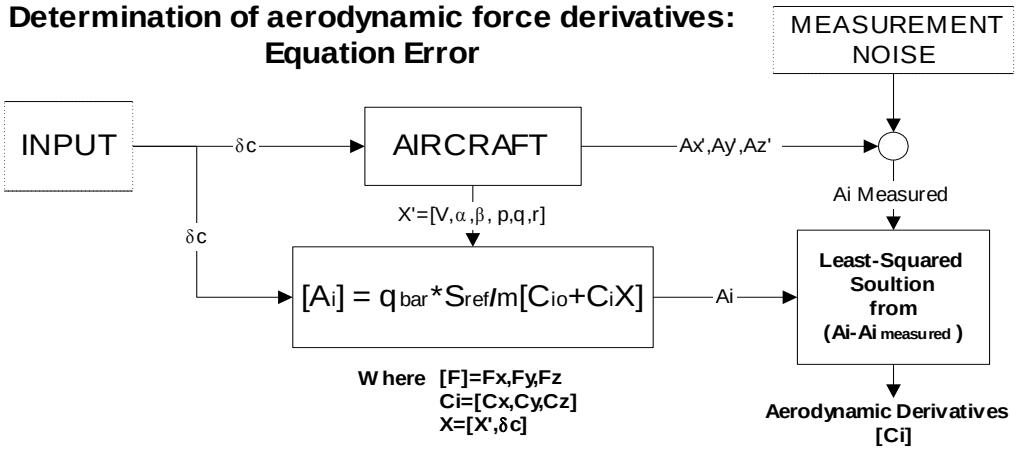

Figure 4. Diagram illustrating computational flow of and equation error estimation.

Figure 5 contains the same estimate of aerodynamics force components above, but using an output method. In the output error case, the model uses model states to compute the model output. This output in addition to measured output is then needed along with model sensitivities in the parameter estimator.

The Maximum Likelihood method is similar to the output error method, but uses the condition probability density function, also called the log likelihood function, as the cost function, Where output error methods typically use a cost function similar to the mean-squared error between estimated output and measured output. The basic principle of the maximum likelihood method is to provide estimates that will "most likely" yield the measure output.

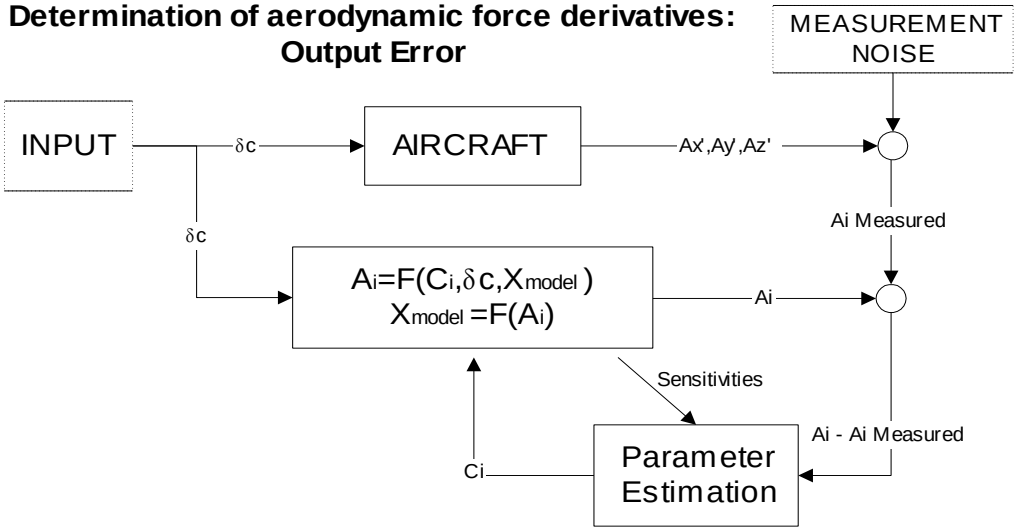

Figure 5. Diagram illustrating computational flow of and output error estimation.

Automated Fidelity Testing (AFT)

AFT is a batch-mode operation of a simulation that performs programmed maneuvers then compares results with defined data. Typically these defined data are acceptance criteria data that have been obtained from flight test data. Maneuvers are performed simple pilot models that have been adjusted to meet maneuver requirements. AFT typical included maneuvers such as accelerations,

decelerations, climbs, stalls, spins, doublets, take-offs, landings, etc. Automated-Fidelity Testing can a valuable tool in the development and long-term support of a simulation model when used appropriately. It can be used for both validation and verification of simulation models. When analyzing results from AFT, the engineer must assess the quality of the performed maneuver. Sometimes AFT can result in maneuvers that are flown much better than they were when the "truth" data being used for comparison were collected. All AFT maneuver input and execution must match the maneuvers that were flown during flight tests, otherwise AFT comparisons with data from the flight tests will be meaningless.

Desk-Top Piloted Simulation (DPS)

Desktop-Piloted Simulation is an evaluation technique that can save time and money during a flight model development effort. Recent advances in simulation tools have made desktop pilot simulation an affordable reality. In the past, and in some cases in the present, flight models are developed and validated without being flown in real-time. Many of these models are intended for flight training devices and flight simulators and are not flown in real-time until integrated with lab or trainer hardware. This can make for a bad situation. Batch-mode checks of the flight model do not guard against discontinuities in the model. Therefore if discontinuities exist, they are revealed once the model is implemented with the hardware and flown in real time. Much time can be spent rectifying the situation and can sometimes lead to a kludged model. This process occupies hardware assets and can be expensive if lab fees are involved

If the flight model development engineer has the ability to evaluate the model in real-time on the same computer being used for model development, these issues can be resolved before hardware integration. Another advantage in using desktop-piloted simulation during flight model development is the ability to "fly" complicated maneuvers that are difficult to run in a batch mode, thus allowing for a more comprehensive validation effort. Using DPS, a flight model engineer could pre-fly an entire simulation test plan prior to having a pilot ever see the simulator. This allows the engineer to verify model continuity and perform preliminary flying qualities and performance check that require manned flight. This approach greatly improves the chances that the first piloted evaluation with the flight simulator will be a success. By preparing the engineer for what to expect from the model, evaluation test plans can focus on particular areas of the flight envelope where pilot opinion is vital thus resulting a reduced requirement for expert pilot evaluation and simulation lab time.

Expert Pilot Evaluation (EPE)

Expert Piloted Evaluation is the evaluation of a flight model or entire simulation by pilots certified to fly the particular aircraft in question. Only pilots with expertise are suited to determine whether or not a simulation behaves like the actual aircraft. Unfortunately, because of typical hardware limitations, such as latency and in some cases the lack of motion queues, a pilot's perception can be skewed. Therefore, comments should be analyzed with recorded simulation response data. This perception problem is the main reason simulation engineers should make use of several different pilots during a simulation evaluation.

Tuning

Tuning is the act of making small, pointed modifications to a model to achieve a desired response. This modeling technique is most often applied to areas of the flight envelope where little flight data exist. Adjusting a model to please a single pilot should not be standard practice. Always attempt to get a second opinion. Once the model is modified, try to have a third pilot perform the final evaluation.

Tuning can also be used to match a prescribed output from flight test data, but can be a risky modeling technique that will lead to an inconsistent, inaccurate model if not done properly. Model tuning should always be performed with discipline and expertise. As with tuning to piloted assessment, the simulation engineer should avoid model modifications given a single discrepancy. A good rule to abide by is the "multi-symptom" rule. Attempt to find at least two symptoms that point to a specific modeling deficiency.

Case Study: Flight Model for a Military Trainer Configuration, Part II

Introduction

A military trainer configuration (Figure 6) flight model development effort was discussed in Part II of the Math Modeling section of the course. As mentioned, the flight model for the Joint Primary Aircraft Training System (JPATS) competitor under went major modification. Wind-tunnel data were collected and implemented to supplement existing data in the model. This case study focuses on the validation and evaluation of the aerodynamics model and illustrates the application of a commonly used validation technique. The study also provides a discussion of how results lead to further model modifications[2].

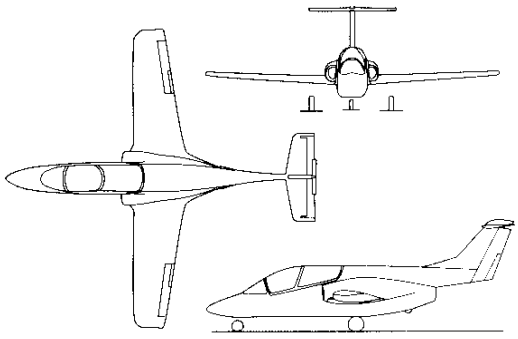

Figure 6. Military trainer three-view diagram

Pitching Moment Validation using Model Isolation Overdrive

During the development of the flight model, analysis of wind-tunnel test results showed a discrepancy in pitching-moment data between wind-tunnel data that were used the simulation aerodynamics model (Convair) and data collected during the dynamic wind-tunnel tests in the Bihrle Applied Research Large Amplitude Multi-Purpose Tunnel (LAMP). As a result, flight test data comparisons were used to determine the appropriate data set to be used in the aerodynamics model. To do this, Model Isolation Overdrive was used to generate simulation output that was suitable for comparing with flight data.

Data from flight test were used to drive the input to the aerodynamics model and extract aerodynamics coefficients. Using measured rate and acceleration data from flight tests, total pitching moment coefficients were computed for comparison with simulation results.

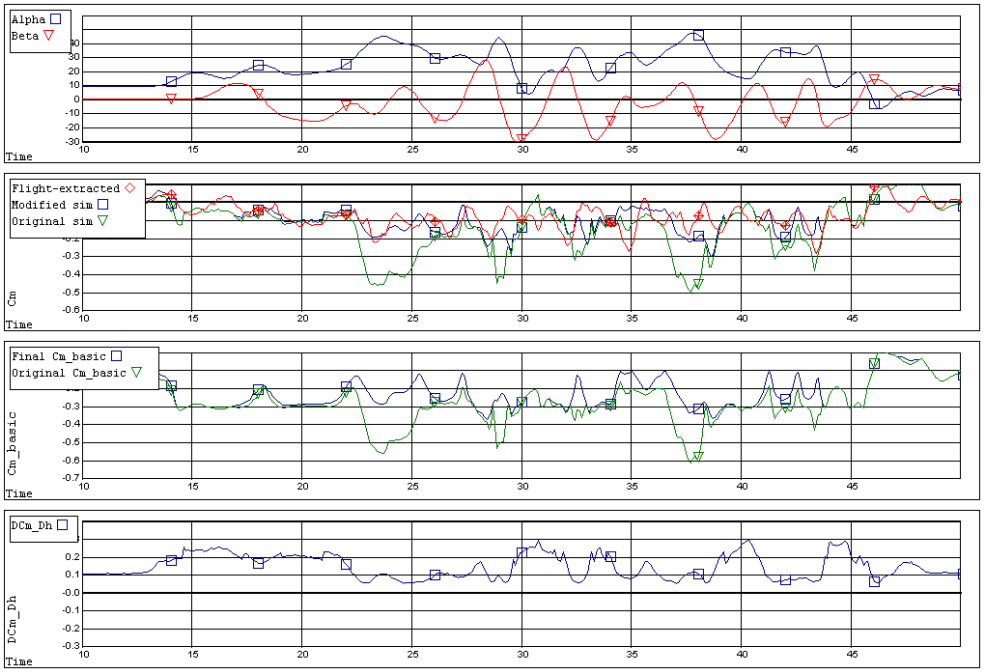

Figure 7. MIO comparison of pitching moment with flight test.

Evaluation of the flight test data revealed that as angle of attack excursions exceeded 30° angle of attack, a repeatable discrepancy between the flight test and simulation predicted pitching moment coefficient occurred (Figure 7). Examination of the pitching moment components showed that the basic airframe pitching moment was responsible for the majority of the simulation pitching moment.

The only other component of consequence, $DCm_{\delta e}$, was much smaller in comparison. Further, the increase in nose down moment consistent with the mismatch was concurrent with the variations in the basic pitching moment data. Evaluation of the test data used in the basic airplane pitch buildup, from Convair tests, show a sharp nosedown break above 30° angle of attack (Figure 8). Comparison with equivalent pitch data taken from the LAMP tests do not exhibit as sharp a break.

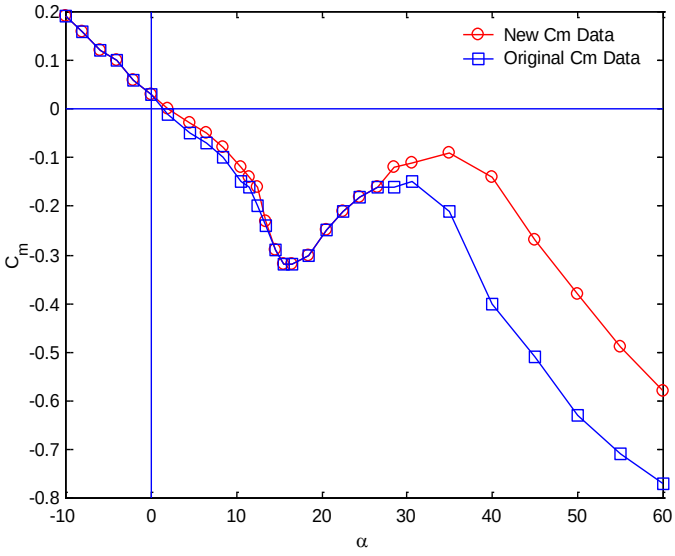

Figure 8. Comparison of new Cm with original Cm.

The original model used the Convair data because of the higher Reynolds number test conditions, but additional influences, potentially blockage or proximity to a tunnel surface apparently adversely affected the higher angle of attack data. When the configuration pitch characteristics seen in the LAMP test data were substituted in the simulation, the pitch matches were greatly improved above 30° angle of attack, as shown in Figure 9.

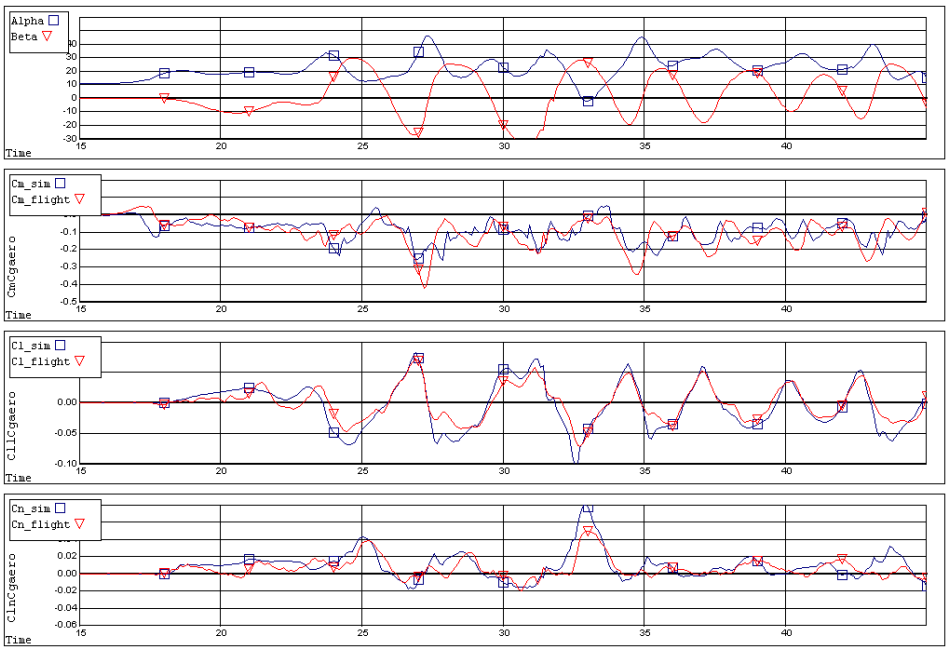

Figure 9. MIO comparison of pitching moment with flight test.

Applications of the Validated Simulation

Recovery Technique Development

Early in the flight test program, spin recoveries were seen to periodically exhibit what was referred to as a “Flick-Roll”. This recovery motion, as shown in Figure 10, resulted when following release of controls the airplane pitched down rapidly during a large oscillation cycle. Typically the airplane would experience a large sideslip excursion at an angle of attack where the lateral stability of the airplane would impose a very large rolling moment. Subsequent roll rates exceeded 250°/sec.

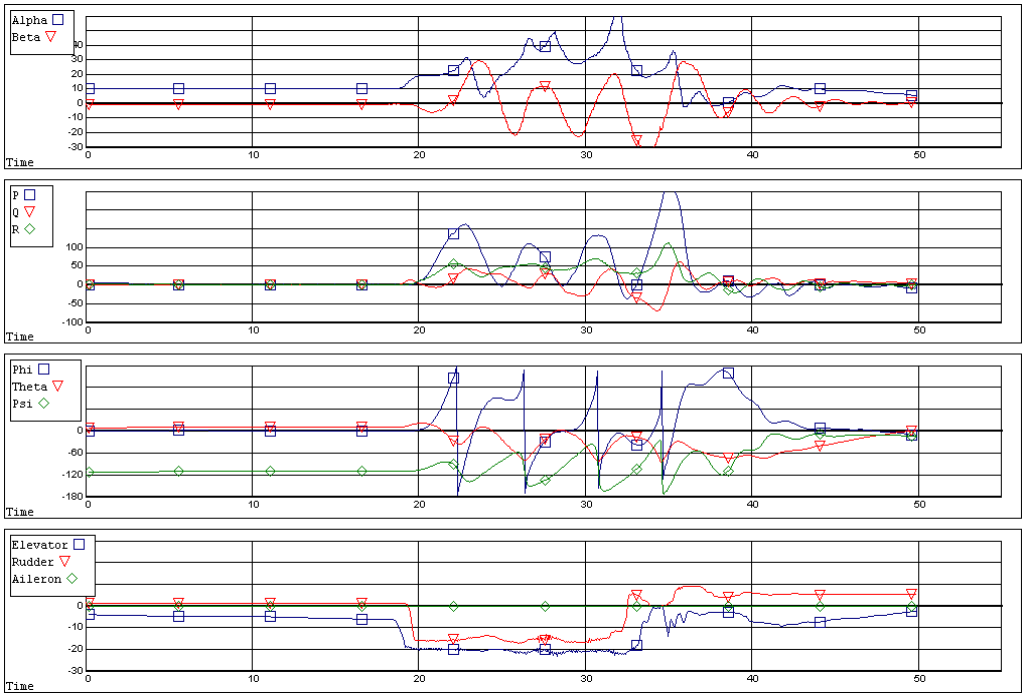

Figure 10. Flight history of the “flick roll” during spin recovery.

The repeated experience of these rates caused concern during the flight test program, since the effect of the high roll acceleration on the wing fuel cells was not known. Following a repetitive occurrence of this maneuver, there was discussion of stopping the test program because of safety issues. Concurrent with this experience, spin recovery procedures were being evaluated with the simulation and for the current recovery procedure, all controls released simultaneously, identical roll rate behavior was observed. Further work with the simulation revealed that maintaining aft stick following the release of the pro-spin rudder reduced the roll oscillations. After the yaw rate subsided, aft stick could be released to bring angle of attack to the normal flight regime. Although this recovery technique required a minimal increase in time to recovery, the reduction in roll rate was judged a significant improvement, and this recovery sequence became the recommended recovery technique. Following acceptance of this control input sequence, the flight test program was permitted to proceed.

Aircraft Spin Characteristic Modification

As the test program continued, the magnitude of the spin oscillations were judged to be unacceptable for a training environment. The motion of the spin was quite uncomfortable with high roll accelerations and pitch angles that oscillated from nose up to pointing straight down, Figure 11. A few months into the test, it was decided that an attempt to reduce the oscillations through a possible external modification would be undertaken. Parametric evaluations using the simulation had shown that the roll due to yaw rate term, C_{lr} , was a key damping characteristic influencing the spin oscillation. The value of

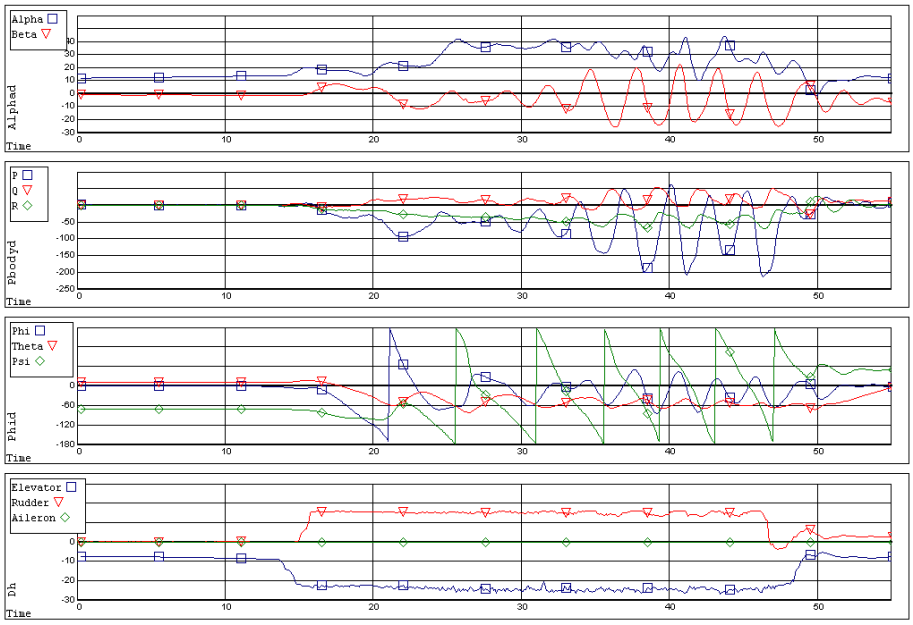

Figure 11. Flight test history of the original spin entry and recovery.

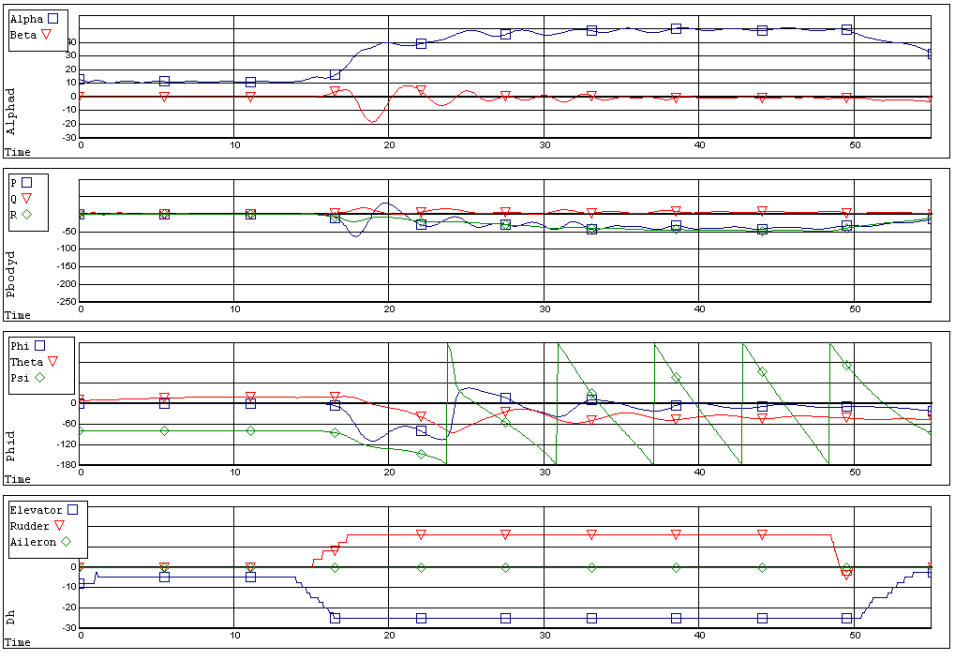

Figure 12. Simulation history with modified roll damping.

this term, as obtained from LAMP tests went unstable in the post-stall region and it was this characteristic that produced the spin oscillations. When the term was modified to remain positive, a much smoother spin resulted (as shown in Figure 12, in comparison to Figure 11). Subscale free spin testing conducted at NASA Langley revealed that the addition of forebody strakes had the effect of reducing the spin oscillations. As a consequence of this, additional tests on these and other modifications were conducted at Convair and LAMP to acquire the required simulation database. LAMP dynamic tests showed the sensitivity to strake position and length on their ability to influence C_{lr} , as shown in the plot of Figure 13.

Limited visualization and component testing suggested that the vorticity shed from the strakes influenced the wing's contribution to this damping term. Spin simulation using the static and dynamic test data indicated that longer strake length would be required in order to minimize the spin oscillations, rather than the shorter length originally selected. These results were verified in flight, where smooth spins required the longer strake. A typical spin obtained with this configuration is shown in the flight test data of Figure 13. This behavior was judged to be a very satisfactory for training with good entry, spin and recovery characteristics and became the designated baseline.

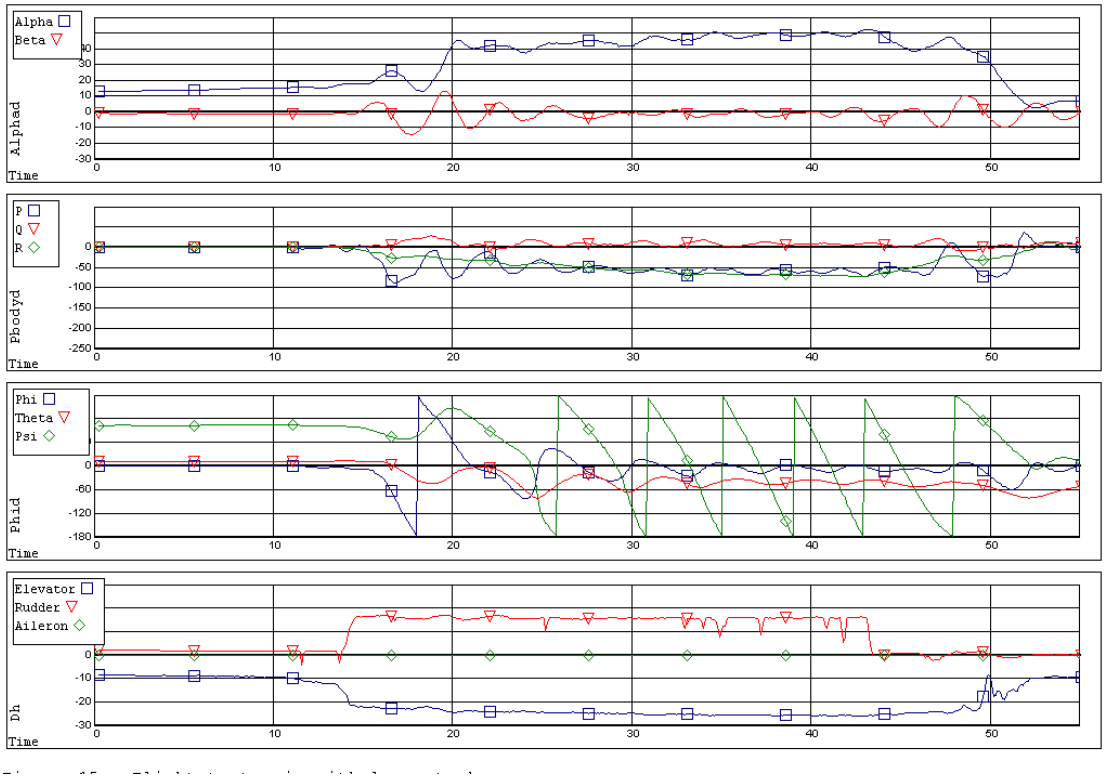

Figure 13. Flight test history of spin with strake modifications.

Summary

Model Isolation overdrive was successfully applied during the validation of the high-angle-of-attack portion of the aerodynamics model. It allowed engineers to determine the source of modeling deficiencies and resolve data discrepancies. The validated simulation then proved vital to the flight test program, where engineers used the simulation to evaluate spin recovery techniques.

The simulation was used to further analyze alternate spin characteristics and perform a parameter study to achieve a desired spin characteristic. The process contributed to a modification to the actual aircraft. Data collected from the flight tests correlated well with the original simulation predictions.

This case study is a good example of the capability of simulation to provide valid predictions of specific high-angle-of-attack motions and characteristics. In this instance the model was used for engineering needs at well as flight test training.

Case Study: F/A-18C/D High-Lift Aerodynamics Model Evaluation

Introduction

The validation work described below was performed by the US Navy Flight Vehicle Simulation Branch in Patuxent River MD and made use of several different methods of model validation. The text provided herein focuses on the validation methodology and provides details pertaining to the lateral directional predictive capability of the model. The effort lead to additional wind-tunnel testing and model modification conducted by Bihrle Applied Research.

The original simulation of the F/A-18 A/B (Figure 14) was received by the Navy from McDonnell-Douglas Aerospace (MDA) in 1983 and modified to fit the FVSB standard simulation architecture, known as the Controls Analysis and Simulation Test Loop Environment (CASTLE).[3] Since then, the Navy has made a considerable effort to improve the F/A-18 simulation Up/Auto-aerodynamics model using wind-tunnel data, parameter identification (PID), and adjustment based on pilot flying-qualities assessments.[4,5,6,7] Less attention has been given to the high-lift aerodynamics models.

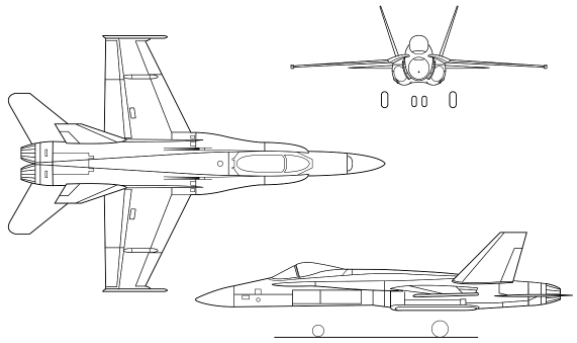

Figure 14. Three-view diagram of the F/A-18A.

The main goal of this effort was to perform a comprehensive evaluation of the F/A-18 simulation high-lift aerodynamics model's capability to accurately predict aerodynamic coefficients for the Fighter-Escort loading (FE) using flight data spanning the normal flight envelope as defined in the United States Navy F/A-18 NATOPS flight manual.[8]

Validation Data

Flight data were collected during a dedicated flight-test program, using F/A-18A BuNo 161744 (SD-102), a Lot V single-seat aircraft. The test article was representative of a production aircraft and was equipped with a Quick Installation Data System (QIDS) package to record variables from the 1553 MUX bus on magnetic tape.[9]

Data for this effort were collected in the Fighter-Escort (FE) loading in the full-flaps (PA) and half-flaps (PA1/2) configurations. In the PA configuration, the trailing-edge flaps (TEF) are drooped to 45° and the ailerons are drooped to 42°. In the PA1/2 configuration, the TEF and ailerons are both drooped to 30°. Data were collected at nominal angles of attack of 6˚, 8.1˚ (on-speed), 10˚, and 12˚ at 5,000 ft altitude in both PA and PA1/2 configurations. Data were also collected with roll- and yaw-control augmentation off (known as CAS/DEL/DEL mode) in the PA1/2 configuration. Maneuvers flown during the data collection flights included pitch, roll, and yaw 3-2-1-1s and Steady-Heading Sideslips (SHSS). The 3-2-1-1 is a variable duration dual cycle square wave doublet designed to have broad spectral content and yet be easy for the pilot to fly.[10] A total of 19,431 data points, collected at a 20 Hz sample rate, were available, with 8,478 data points in the PA configuration and 10,953 in the PA 1/2 configuration.

Flight data were analyzed for consistency among redundant data sources then evaluated for kinematic consistency. In cases where the data were not consistent, a maximum-likelihood algorithm was used to identify flight data correction parameters.[11] Biases were identified and applied to angular-rate and linear-accelerometer measurements. Angle-of-attack measurements required scaling corrections. In addition to bias and scale corrections, measurement delays were identified in angle-of-attack, airspeed, angular-rate, and the linear-acceleration measurements. Corrections made to the data were relatively small, but improved data consistency.[12]

Simulation Aerodynamics Model Structure

The FVSB F/A-18A-D simulation high-lift aerodynamics model consists of a detailed nonlinear-model-component build up based on look-up tables created from wind-tunnel data with minor adjustments based on flight data. The equation set below contains the model structure for both full- and half-flap configurations.

Two baseline configurations are implemented in the high-lift model. The PA baseline configuration features ailerons drooped to 42°, TEF drooped to 45°, and Leading-Edge Flaps (LEF) at 15°, with all remaining control surfaces undeflected. The PA1/2 baseline features ailerons and TEF drooped to 30° with LEF at 15°. Each model assumes a standard FE loading. Various increments for centerline tank, interdiction loading, and two-seat canopy are added to the basic model as appropriate.

Validation Methodology

Two approaches were used to evaluate the high-lift model. Direct aerodynamic coefficient comparisons were performed for each of the maneuvers to assess the overall predictive ability of the model. Nonlinear-model comparisons provided detailed information pertaining to specific discrepancies in the model. The following sections describe each process.

Direct Coefficient Comparison

Aerodynamic coefficients extracted from flight data were compared with corresponding coefficients predicted by the simulation model. Additional statistical figures of merit were used to categorize different types of errors and the overall level of fidelity of the simulation aerodynamics model

Aerodynamic coefficients were extracted from the corrected flight data using equation set (1). All moment coefficients were referenced to 25% mean aerodynamic chord. Estimates of thrust were generated by the simulation's engine model using MIO. Because of the lack of a properly instrumented engine and uncertainty in the thrust estimates, the simulation's drag model was not assessed. This uncertainty was also propagated to a lesser extent to the reconstructed lift and pitching moment.

$$
\begin{aligned}
C_L &= C_{L_o}(\alpha) + \Delta C_L(\alpha, \delta_{LEF_l}) + \Delta C_L(\alpha, \delta_{LEF_r}) + \Delta C_L(\alpha, \delta_{TEF}) + \Delta C_L(\alpha, \delta_{Stab_l}) + \Delta C_L(\alpha, \delta_{Stab_r}) + \Delta C_L(\alpha, \delta_{Ail_l}) \\
&\quad + \Delta C_L(\alpha, \delta_{Ail_r}) + \Delta C_L(\alpha, \delta_{Rud_l}) + \Delta C_L(\alpha, \delta_{Rud_r}) + \Delta C_L(\alpha, \delta_{Rudtoe_l}) + \Delta C_L(\alpha, \beta) + \frac{\bar{c}}{2V}\left(C_{Lq}(\alpha)q + C_{L\dot{\alpha}}(\alpha)\dot{\alpha}\right) \\
&\quad + C_{L_{\delta SB}}(\alpha,)\delta_{SB} + \Delta C_L(\alpha, h - h_g, \delta_{Stab}) + \Delta C_{L_{GearPos}}(\alpha,)GearPos + \Delta C_{L_{Loading}} \\
C_D &= C_{D_o}(\alpha) + \Delta C_D(\alpha, \delta_{LEF_l}) + \Delta C_D(\alpha, \delta_{LEF_r}) + \Delta C_D(\alpha, \delta_{TEF}) + \Delta C_D(\alpha, \delta_{Stab_l}) + \Delta C_D(\alpha, \delta_{Stab_r}) + \Delta C_D(\alpha, \delta_{Ail_l}) \\
&\quad + \Delta C_D(\alpha, \delta_{Ail_r}) + \Delta C_D(\alpha, \delta_{Rud_l}) + \Delta C_D(\alpha, \delta_{Rud_r}) + \Delta C_D(\alpha, \delta_{Rudtoe_l}) + C_{D_{\delta SB}}(\alpha,)\delta_{SB} + \Delta C_D(\alpha, h - h_g, \delta_{Stab}) \\
&\quad + \Delta C_{D_{GearPos}}(\alpha,)GearPos + \Delta C_{D_{Loading}} \\
C_m &= C_{m_o}(\alpha) + \Delta C_m(\alpha, \delta_{LEF_l}) + \Delta C_m(\alpha, \delta_{LEF_r}) + \Delta C_m(\alpha, \delta_{TEF}) + \Delta C_m(\alpha, \delta_{Stab_l}) + \Delta C_m(\alpha, \delta_{Stab_r}) + \Delta C_m(\alpha, \delta_{Ail_l}) \\
&\quad + \Delta C_m(\alpha, \delta_{Ail_r}) + \Delta C_m(\alpha, \delta_{Rud_l}) + \Delta C_m(\alpha, \delta_{Rud_r}) + \Delta C_m(\alpha, \delta_{Rudtoe_l}) + \Delta C_m(\alpha, \beta) + \frac{\bar{c}}{2V}\left(C_{mq}(\alpha)q + C_{m\dot{\alpha}}(\alpha)\right) \\
&\quad + C_{m_{\delta SB}}(\alpha,)\delta_{SB} + \Delta C_m(\alpha, h - h_g, \delta_{Stab}) + \Delta C_{m_{GearPos}}(\alpha,)GearPos + \Delta C_{m_{Loading}} \\
C_Y &= C_{Y_o}(\alpha, \beta) + C_{Y_{\Delta\delta Stab}}(\alpha, \beta)\Delta\delta_{Stab} + \Delta C_Y(\alpha, \Delta\delta_{Ail_l}) + \Delta C_Y(\alpha, \Delta\delta_{Ail_r}) + \Delta C_{Y_{\bar{\delta}_{Rud}}}(\alpha)\bar{\delta}_{Rud} + \Delta C_Y(\alpha, \beta, \delta_{Rudtoe}) \\
&\quad + \frac{b}{2V}\left(C_{Yp}(\alpha)p + C_{Yr}(\alpha)r\right) + \Delta C_{Y_{Loading}} \\
C_l &= C_{l_o}(\alpha, \beta) + C_{l_{\Delta\delta Stab}}(\alpha, \beta)\Delta\delta_{Stab} + \Delta C_l(\alpha, \Delta\delta_{Ail_l}) + \Delta C_l(\alpha, \Delta\delta_{Ail_r}) + \Delta C_{l_{\bar{\delta}_{Rud}}}(\alpha)\bar{\delta}_{Rud} + \Delta C_l(\alpha, \beta, \delta_{Rudtoe}) \\
&\quad + \frac{b}{2V}\left(C_{lp}(\alpha)p + C_{lr}(\alpha)r\right) + \Delta C_{l_{Loading}} \\
C_n &= C_{n_o}(\alpha, \beta) + C_{n_{\Delta\delta Stab}}(\alpha, \beta)\Delta\delta_{Stab} + \Delta C_n(\alpha, \Delta\delta_{Ail_l}) + \Delta C_n(\alpha, \Delta\delta_{Ail_r}) + \Delta C_{n_{\bar{\delta}_{Rud}}}(\alpha)\bar{\delta}_{Rud} + \Delta C_n(\alpha, \beta, \delta_{Rudtoe}) \\
&\quad + \frac{b}{2V}\left(C_{np}(\alpha)p + C_{nr}(\alpha)r\right) + \Delta C_{n_{Loading}}
\end{aligned}
\tag{1}
$$

$$C_x = \frac{m}{\bar{q}S}\left(F_x - F_{x_{Eng}}\right)$$
$$C_y = \frac{m}{\bar{q}S}\left(F_y - F_{y_{Eng}}\right)$$
$$C_z = \frac{m}{\bar{q}S}\left(F_z - F_{z_{Eng}}\right)$$
$$C_l = \frac{m}{\bar{q}Sb}\left(M_x - M_{x_{Eng}} - F_y\Delta z_{cg} + F_z\Delta y_{cg}\right)$$
$$C_m = \frac{m}{\bar{q}S\bar{c}}\left(M_y - M_{y_{Eng}} + F_x\Delta z_{cg} - F_z\Delta x_{cg}\right)$$
$$C_n = \frac{m}{\bar{q}Sb}\left(M_z - M_{z_{Eng}} - F_x\Delta y_{cg} + F_y\Delta x_{cg}\right)$$

with

$$C_L = C_x \sin\alpha - C_z \cos\alpha$$
$$C_D = -C_x \cos\alpha - C_z \sin\alpha$$

where

$$F_X = mA_x$$
$$F_Y = mA_y$$
$$F_Z = mA_z$$
$$M_x = \dot{p}I_{xx} - \dot{q}I_{xy} - \dot{r}I_{xz} + qr\left(I_{zz} - I_{yy}\right) + \left(r^2 - q^2\right)I_{yz} - pqI_{xz} + rpI_{xy}$$
$$M_y = -\dot{p}I_{xy} + \dot{q}I_{yy} - \dot{r}I_{yz} + rp\left(I_{xx} - I_{zz}\right) + \left(p^2 - r^2\right)I_{xz} - qrI_{xy} + pqI_{yz}$$
$$M_z = -\dot{p}I_{xz} - \dot{q}I_{yz} + \dot{r}I_{zz} + pq\left(I_{yy} - I_{xx}\right) + \left(q^2 - p^2\right)I_{xy} - rpI_{yz} + qrI_{xz}$$

Simulation-predicted coefficients were obtained by driving the high-lift-aerodynamics model with flight data without propagating the equations of motion. The results of this process are simulation-predicted aerodynamic force and moment coefficients for a *specific* measured aircraft state. These were plotted along with the flight-test reconstructed coefficients for evaluation.

The coefficient comparisons were assessed by visual inspection and by using Theil statistics, equations (2) and (3). Theil's inequality coefficient, equation (2), is a normalized measure of agreement between two signals.[13] It is the RMS error between the two signals, normalized by the combined RMS value of both signals. The inequality coefficient is always between zero and one, with zero representing an exact match and one representing the "worst" case match. Worst case matches are obtained when one signal is zero and the other signal is nonzero, or when the signals are perfectly negatively correlated.

$$U = \frac{\sqrt{\frac{1}{N}\sum_{i=1}^{N}\left(Y_i - \hat{Y}_i\right)^2}}{\sqrt{\frac{1}{N}\sum_{i=1}^{N}Y_i^{\,2}} + \sqrt{\frac{1}{N}\sum_{i=1}^{N}\hat{Y}_i^{\,2}}} \qquad (2)$$

The inequality coefficient can be decomposed into bias, variance, and covariance proportions of inequality as in equation set (3). The error proportions are normalized such that each proportion is between zero and one and the sum of the three proportions is unity. Each of the error proportions provides insight to the source of error between the signals. The bias proportion indicates how much of the error can be attributed to a bias between the two signals.

$$U_{Bias} = \frac{\left(\bar{Y} - \bar{\hat{Y}}\right)^2}{\frac{1}{N}\sum_{i=1}^{N}\left(Y_i - \hat{Y}_i\right)^2}$$

$$U_{Var} = \frac{\left(\sigma - \hat{\sigma}\right)^2}{\frac{1}{N}\sum_{i=1}^{N}\left(Y_i - \hat{Y}_i\right)^2} \qquad (3)$$

$$U_{Cov} = \frac{\left(2(1-\rho)\sigma\hat{\sigma}\right)^2}{\frac{1}{N}\sum_{i=1}^{N}\left(Y_i - \hat{Y}_i\right)^2}$$

where

$$\bar{Y} = \frac{1}{N}\sum_{i=1}^{N} Y_i$$

$$\sigma = \sqrt{\frac{1}{N}\sum_{i=1}^{N}\left(Y_i - \bar{Y}\right)^2}$$

$$\rho = \frac{\frac{1}{N}\sum_{i=1}^{N}\left(Y_i - \bar{Y}\right)\left(\hat{Y}_i - \bar{\hat{Y}}\right)}{\sigma\hat{\sigma}}$$

The variance proportion is a measure of how much of the error is correlated with the two signals, i.e. is attributable to a scaling difference. The covariance proportion is a measure of how much of the difference is uncorrelated with the signals. Typically this is a result of random variations (noise), but it can also be caused by model structure errors.

This technique yields an overall view of the simulation model fidelity, and is helpful in identifying gross errors. However, it provides only limited information pertaining to error sources. A more detailed approach is required to identify specific sources of error.

Nonlinear Model Comparison

Equation-error identification techniques were used to identify nonlinear models from the flight data and simulation-predicted coefficients.[14] The equation-error technique is time-independent, therefore maneuvers were concatenated and analyzed as ensembles of data points to enhance information content. Nonlinear spline models for the aerodynamic coefficients were identified using stepwise regression.[15] Comparison of these models allowed for a detailed evaluation of specific sources of error.

The form of the longitudinal models was postulated as in equation (4), and the lateral-directional models as in equation (5). Previous work has shown that the lateral-directional aerodynamics are sensitive to TEF deflection, therefore independent models were identified for the PA and PA1/2 configuration maneuvers.[5] The TEF and drooped aileron deflections were modeled as perturbations from the nominal deflections. Nominal TEF and drooped-aileron deflections were 45° and 42° respectively for the PA configuration, and 30° each for the PA1/2 configuration. The TEF term that appears in equation (4) was only used for the PA model, as the PA1/2 data had no significant off-nominal TEF deflections.

The baseline longitudinal model terms, $C_{L_o}(\alpha)$ and $C_{m_o}(\alpha)$, were modeled as first-order splines. The remaining model terms were modeled as zeroth-order splines, i.e. piecewise constants. Each of the model terms were allowed to vary with angle of attack, by specifying spline knots at various angles of

attack from 4° to 13°. Each coefficient term and spline knot in the model is associated with a particular regressor in the stepwise-regression procedure. Regressors are selected for inclusion in the model based on the significance of the regressor in the model. Regressors were retained if the partial F-statistic was greater than 7.0. This single criterion, which indicates a regressor's significance in the model, allows a number of marginally acceptable parameters to be included in the identified models. Since the purpose of the model-identification step was to indicate the basic causes of the observed modeling errors, their general magnitude and possible angle-of-attack functionality, a more detailed analysis was not considered appropriate. A detailed model identification includes more stringent selection criteria to identify an optimal model but avoid over-parameterization.[14]

$$C_a = C_{a_o}(\alpha) + C_{a_q}{}'(\alpha) q \frac{\bar{c}}{2V} + C_{a_{\delta\bar{H}}}(\alpha)\delta\bar{H} + C_{a_{\delta\bar{T}\bar{E}\bar{F}}}(\alpha)\left(\delta\bar{T}\bar{E}\bar{F} - \delta\bar{T}\bar{E}\bar{F}_{nom}\right) + C_{a_{\delta\bar{A}}}(\alpha)\left(\delta\bar{A} - \delta\bar{A}_{nom}\right) + C_{a_{|\beta|}}(\alpha)|\beta| \qquad a = L, D, m \tag{4}$$

$$C_a = C_{a_\beta}(\alpha)\beta + \left(C_{a_p}(\alpha)p + C_{a_r}(\alpha)r\right)\frac{b}{2V} + C_{a_{\delta Ad}}{}'(\alpha)\delta Ad + C_{a_{\delta\bar{H}}}(\alpha)\delta\bar{R} \qquad a = Y, l, n \tag{5}$$

Because of the high correlation between differential stabilator and aileron, it was not possible to identify independent model terms for these parameters. In this analysis, differential-aileron derivatives contained inherent differential stabilator effects as well. A similar correlation existed between pitch rate and $\dot{\alpha}$. Once again, a combined derivative was identified which incorporated both pitch-rate and $\dot{\alpha}$ effects. The combined derivative terms are signified with primes in the model structure. A similar problem existed with the angle-of-attack, average leading-edge-flap (LEF), and flared-rudder terms. The F/A-18 control system scheduled average LEF and flared rudder with angle of attack in both PA and PA1/2 modes, leading to high correlation between these parameters. Combined scheduled LEF and flared-rudder effects are inherent in the identified model terms.

A unique aspect of this comparison technique was the identification of nonlinear models from the simulation-predicted coefficients, as opposed to extracting the models directly from the simulation data tables and source code. Previous efforts have compared linear models extracted from flight data to linear models extracted directly from the simulation using perturbation methods.[16]

The nonlinear-model-comparison technique was chosen to ensure that similar quantities were being compared. Given the high levels of correlation among some states and control surfaces in the flight data, it was necessary to identify several combined or equivalent derivatives and include inherent surface deflection effects in the flight-data models. Direct comparison of these equivalent and inherent model terms to the simulation models is difficult. By using the same model structure and measured inputs to identify the simulation models as were used to identify the flight models, these inherent effects are automatically included in both models. Spot checks of several of the identified simulation model terms verified that these terms were consistent with the values extracted from the simulation source code and data tables.

Evaluation Results

Direct Coefficient Comparison

An example of a typical direct coefficient comparison is presented in Figure 15. The predicted side-force, rolling- and yawing-moment coefficients are presented for a PA1/2 CAS/DEL/DEL yaw 3-2-1-1 maneuver. The plot presents several pieces of information. The actual coefficient time sequences are plotted in the main axis. Below the main axis, the residual sequence is plotted. To the right of the main axis, a graphical representation of the inequality coefficient and proportions of inequality is presented.

The first bar represents the inequality coefficient, while the narrow bars represent the bias, variance, and covariance error proportions respectively. Using this information, a rough estimate of the simulation's predictive capability *for a particular maneuver* was determined. In this particular case, dynamic overshoots were apparent in each coefficient. Note that the variance proportions were fairly high in each case, which indicates scaling type errors.

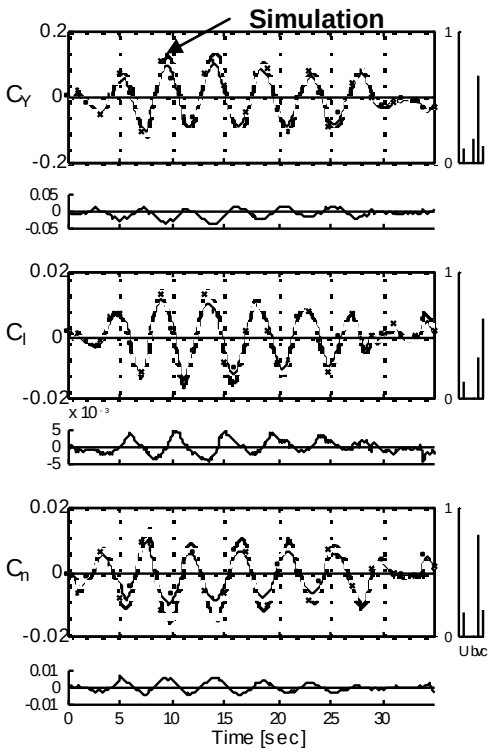

Figure 15. Typical comparison plot from the F/A-18 aerodynamics model validation effort.

Lateral-Directional Comparisons

The simulation generally over-predicted dynamic peaks in the lateral-directional coefficient sequences. The simulation predicted side-force coefficient best, followed by yawing-moment and rolling-moment coefficients. The best side-force and yawing-moment coefficient comparisons were obtained during yaw 3-2-1-1 inputs. Roll 3-2-1-1 inputs resulted in the best rolling-moment coefficient comparisons. All the lateral-directional coefficient comparisons showed significant dynamic errors for the 12° nominal angle-of-attack maneuvers.

Examination of inequality coefficients for the PA1/2 side-force and rolling-moment comparisons were lower on average than the PA comparisons, while the yawing-moment inequality coefficient was identical. This is in contrast to the longitudinal coefficient results, where the PA1/2 comparisons were generally worse than the PA.

In general, the error was evenly distributed between bias, variance, and covariance proportions. This indicated that a number of different error sources were responsible. The larger errors in the lateral-directional coefficient comparisons, as well as the tendency towards dynamic overshoots as opposed to constant biases, indicated that the lateral-directional high-lift model was less accurate than the longitudinal model.

Nonlinear-Model Comparison

The identified lateral directional models, based on the model structure in equation (4), are plotted versus angle of attack for the PA1/2 configuration in Figure 16 and the PA configuration in Figure 17. Error bars represent the 95% confidence bounds using the large-sample assumption, i.e. they depict twice the estimated parameter standard error.[17] The zeroth-order spline-model terms were represented by plotting the spline value at the midpoint of each knot range. In these cases the connecting lines are for illustrative purposes only and do not indicate higher-order functionality. Note that in some cases, the stepwise regression algorithm did not identify model terms for $\alpha < 5°$ (see, for example, C_{y_r} in Figure 16). In these cases, the model term is plotted as zero but is not interpreted as an identified value of zero.

Several significant model deficiencies were identified in the lateral-directional model. The simulation model was generally more stable than indicated by the flight-test models in both PA1/2 (Figure 16) and PA (Figure 17) configurations. The dihedral stability C_{l_β} and the directional stability C_{n_β} were over-predicted by the simulation. The simulation model also showed a trend towards increasing dihedral stability with increasing angle of attack in both configurations. This trend was matched by the PA1/2 flight data model, however the PA flight data model indicated C_{l_β} was nearly constant with angle of attack. Overall trends in directional stability were similar between flight-data and simulation models. The simulation over-predicted side-force due to sideslip in both PA and PA1/2 configurations, however the trends with angle of attack were similar.

Control effectiveness was generally over-predicted by the simulation for both flap configurations. Side force due to rudder, rolling moment due to aileron, and yawing moment due to rudder were all over-

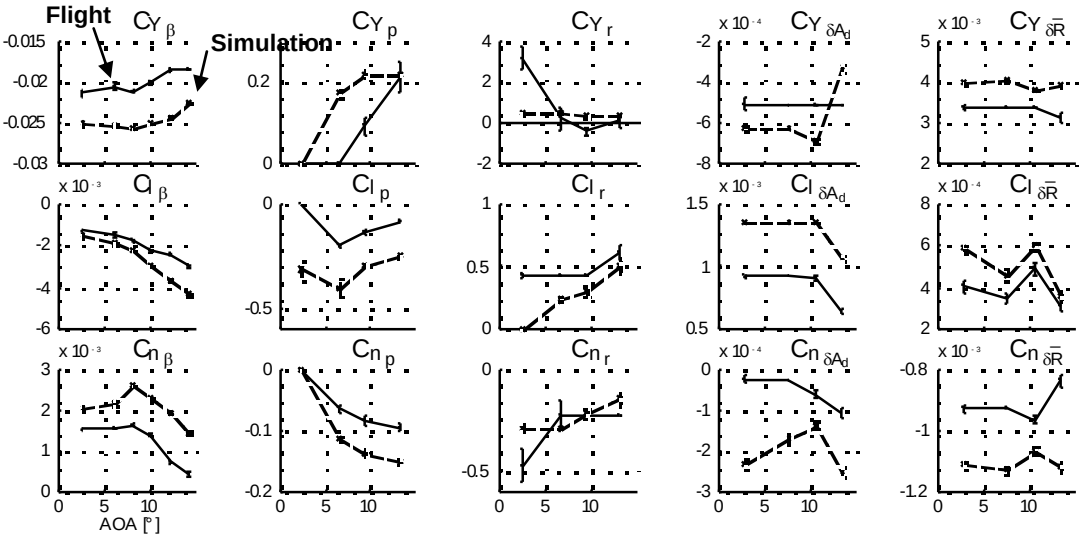

Figure 16. Nonlinear lateral-directional model comparison for PA 1/2configuration

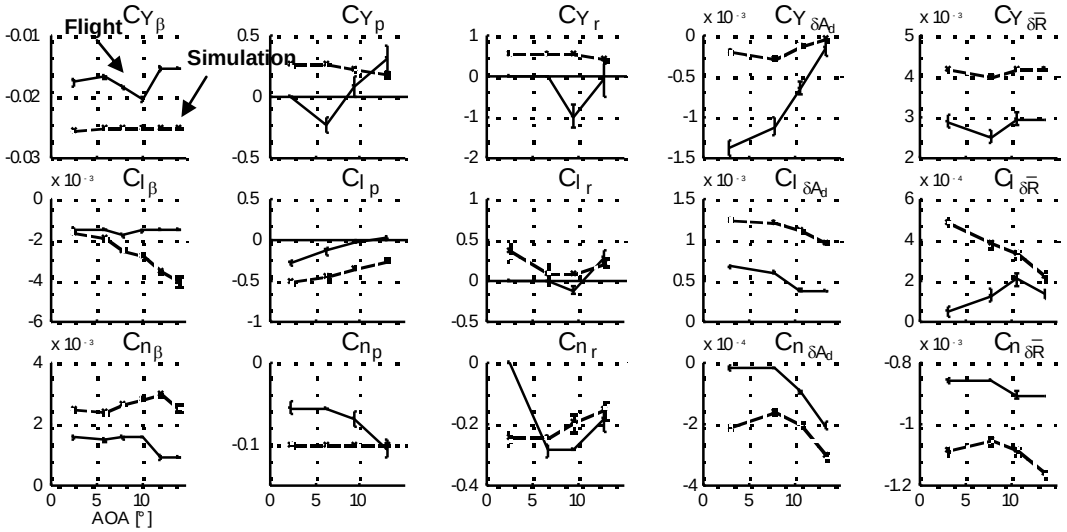

Figure17. Nonlinear lateral-directional model comparison for PA configuration

predicted by the simulation. In some cases these mismatches were close to 100% of the flight-data predicted magnitude, however both flight-test and simulation models displayed similar trends with angle of attack. More discrepancy was noted in the cross-axis control derivatives. The adverse yaw term, $Cn_{\delta A}$, was over-predicted by the simulation in both configurations. The PA1/2 configuration $Cl_{\delta R}$ model terms showed similar trends, with the simulation tending to under-predict the magnitude slightly. In the PA configuration, the flight-test and simulation models indicated opposite trends in Cl_{dR} with angle of attack for $\alpha < 10°$.

Significant discrepancies were noted in the roll-rate damping terms. Flight-test and simulation roll damping estimates showed similar trends with angle of attack, however Cl_p was over-predicted by the simulation in both the PA and PA1/2 configurations. One interesting result was the prediction of nearly neutral to unstable roll damping above 10° α in the PA configuration flight-test model. The cross-axis

damping term C_{n_p} was over-predicted by the simulation model in both flap configurations. The simulation model side-force due to roll (C_{Y_p}) was approximately 0.25 in both configurations, whereas the flight-test models predicted negative C_{Y_p} for $\alpha < 10°$ and positive C_{Y_p} for $\alpha > 10°$.

The yaw-damping term C_{n_r} compared well in both flap configurations with some variation in the low-angle-of-attack range. This variation was attributed to uncertainty in the identified flight models. The flight identified C_{Y_r} and C_{l_r} terms showed considerable variability in angle of attack and significant differences between the PA and PA1/2 configuration results, making these terms difficult to evaluate.

It is possible that observed discrepancies in the cross-axis control and cross-axis damping terms were not a result of simulation modeling deficiencies, but were a result of poor identification of these terms from flight data. These terms are typically difficult to identify, as they generally are of limited significance in the overall model. In these cases, the nonlinear-model analysis results were used to indicate potential problems with these model terms, without explicitly quantifying them.

Lateral-Directional Model Modification and Validation

Further investigation of the evaluation results of the evaluation of the powered approach model lateral and directional characteristics indicated a need for expanded model functionality. A close look at the coefficient build-up of the lateral-direction coefficients in the F/A-18 model in equation (1) reveals a lack of leading-edge flap and sideslip effect on aileron. Investigation of flight control block diagrams and data from the flight tests revealed leading-edge deflections is scheduled with angle of attack and were not fixed but were scheduled with angle of attack. Figure 18 contains a plot of leading-edge flap deflections measured during the validation collection flights. With this information, it was hypothesized that the poor predictions of rolling moment coefficient by the simulation were due to lack functionality in aileron effectiveness.

A short wind-tunnel test was designed and conducted to determine the effects of leading edge deflection and sideslip angle on aileron effect. Wind-tunnel data revealed a distinct effect of leading-edge flap deflection on aileron effectiveness and an overall decrease in aileron effectiveness than data in the existing model.

The new aileron data were implemented into the simulation as a four-dimensional lookup table that was a function of aileron deflection, sideslip, leading-edge flap, and trailing-edge flap. Model isolation

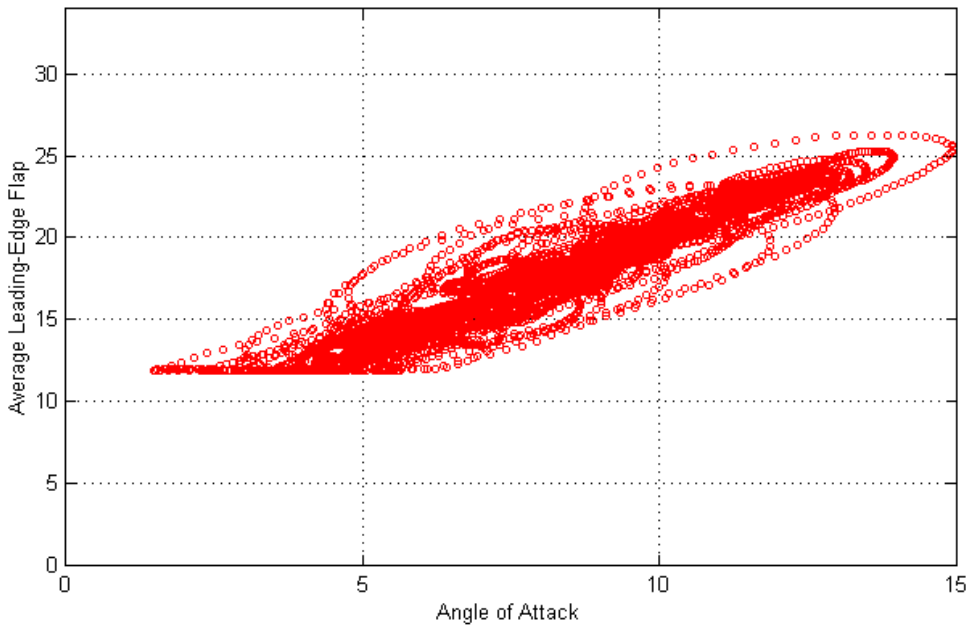

Figure 18. Leading-Edge flap deflections measure during validation data collection flights.

overdrive simulation runs were repeated and showed that the new data improved the fidelity of the aerodynamics model. Figure 19 contains a sample comparison output from the effort.

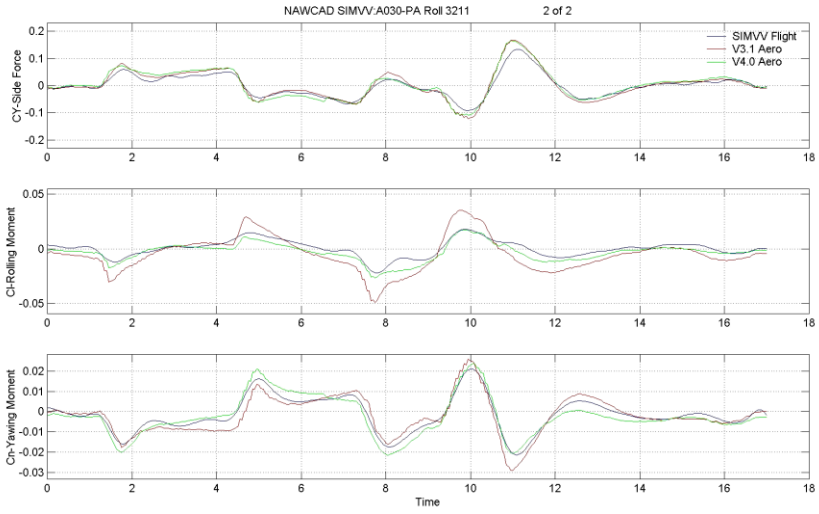

Figure 19. Comparison plot containing new aileron power model

Summary

The use of data from a flight test program designed specifically for simulation validation was a success. Advanced validation methods were implemented and exposed discrepancies. The methods also allowed engineers to identify specific areas of the aerodynamics model that needed improvement. As a result, a wind-tunnel test was designed by the Navy to address specific needs of the model. The data from the wind tunnel were then used to modify the model and increase its fidelity, as shown through the validation of the modification.

This case provides an excellent example of the use of flight data for validation and alternate data for validation. The data collected during the flight were analyzed for data quality then used for validation, and validation only. Rather than using these data to tweak the model, the model was expanded with a second set of data. In this case, because of budget constraints, the second source of data came from a wind-tunnel test.

Case Study: AV-8BII+ Aerodynamics Model Development

Introduction

Requirements in the development of the Italian Navy's AV-8BII+ Mission Simulator (IMS), Device S2F176, specified a flight model upgrade to existing training simulator models.[18] This case study describes the several key issues in the development and validation effort and will focus on the techniques used to ensure the development of a high-fidelity model.

The IMS Device was to be representative of the radar variant of a CUM 250 AV-8B, designated the AV-8BII+ (Figure 20). The AV-8B II+ possesses a different radome configuration than the night attack aircraft. A specification for acceptance of the trainer was defined based on the AV-8BII+ CUM 250 aircraft that the Italian Navy flies. The AV-8B is a VSTOL (Vertical and Short Take off and Landing) aircraft has three modes of flight, Jet-Born, Semi-jet-born, and wing-born. As the name indicates, jet-born flight occurs when the Roll Royce engine provides virtually all lift required to keep the jet air-born. Nozzle deflections range from approximately 80 to 98 degrees relative to the aircraft body axes with trailing-edge flap extended to over 60 degrees. Flight control is handled by the reaction control system (RCS). The semi-jet-born mode or STOL configuration is used during short take-offs and short landings. Nozzle and flap deflections range between 40 and 70 degrees. RCS control is couple with conventional aerodynamic surface control. The last mode of flight is wing-born flight. During wing-born flight, the AV-8 flies like a conventional aircraft, but maintains the ability to rotate nozzle to gain a tactical advantage during combat maneuvering.

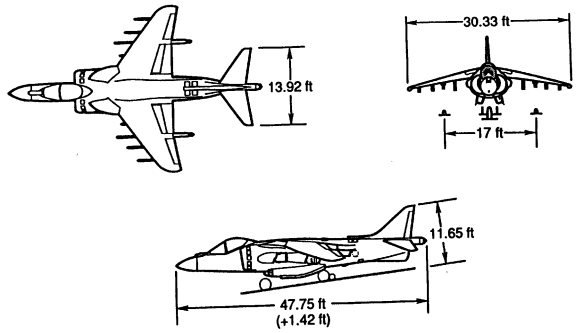

Figure 20. Three-view diagram of the AV-8B II +.

Aerodynamics Model Development

The improved Device S2F176 flight model was constructed using a model structure and data from three existing simulation models, an AV-8B trainer model, and two US Navy Engineering aerodynamics models. During the development effort, the strengths and weaknesses of each of the models were evaluated. As a result, it was decided to use portions of each of the models to create the new aerodynamics model for the IMS.

The basic model structure for the aerodynamics model was borrowed from the two engineering models. The engineering models contained a good representation of AV-8B high-angle-of-attack aerodynamics in addition to a comprehensive database and model structure. The existing trainer model had been modified over the years and contained code modifications to data as well as a number of blending functions to link portions of different regions of the flight model. In contrast, the engineering models offered a continuous model structure, unfortunately it lacked functionality that the trainer model possessed, such as failures, extended store effects, and ground effects. Therefore, functionality from the trainer model was incorporated into the new model.

Model Validation

During the development of the flight model, four validation techniques were used to evaluate the simulation, Automated Fidelity Testing (AFT), Direct Simulation Overdrive (DSO), Desktop Piloted Evaluation (DPS), and Expert Pilot Evaluation (EPE). The application of each of these techniques required a certain level of expertise and familiarity with the data being used to validate the model.

Evaluation Using Automated Fidelity Testing (AFT)

As mentioned in a previous section, AFTs perform maneuvers using autopilots and automated input. The technique can be used to document simulator response to an input or it can be used to compare simulator response to accepted "truth" data.

If AFT is to be used for flight model acceptance, particular attention must be paid to the execution of the AFT maneuver. If the maneuver is not performed correctly the results and reduced data from the results may not be suitable for comparison to "truth" data.

A good example of this is the evaluation of roll performance during the AV-8B flight model development. Flying qualities reports contained data pertaining to roll performance in charts depicting maximum roll rate, Time-to 90, and maximum adverse sideslip. The charts contained data indicating the initial angle of attack for the maneuver, but gave little description on how the maneuver was performed. The description of the maneuver indicated the data were collected during full high-speed-stop lateral stick rolls. The high-speed stop is a mechanical detent in the lateral control of the AV-8B.

The execution of the AFT to compare roll performance seemed simple enough. Trim the simulation to the desired condition; apply lateral stick to the high-speed stop until a 360 roll is executed. The AFT data were reduced then compared to "truth" data. The results were not good, showing that the simulation roll rates were out of tolerance and higher than the real aircraft. At first thought one would assume the simulation was wrong and adjust the roll due to aileron until the AFT cases were in tolerance. In this case, that practice would have led to an inaccurate model.

Further investigation led engineers to analyze flight data histories of several of the roll maneuvers used to create the charts. Figure 21 shows an example of such data.[19]

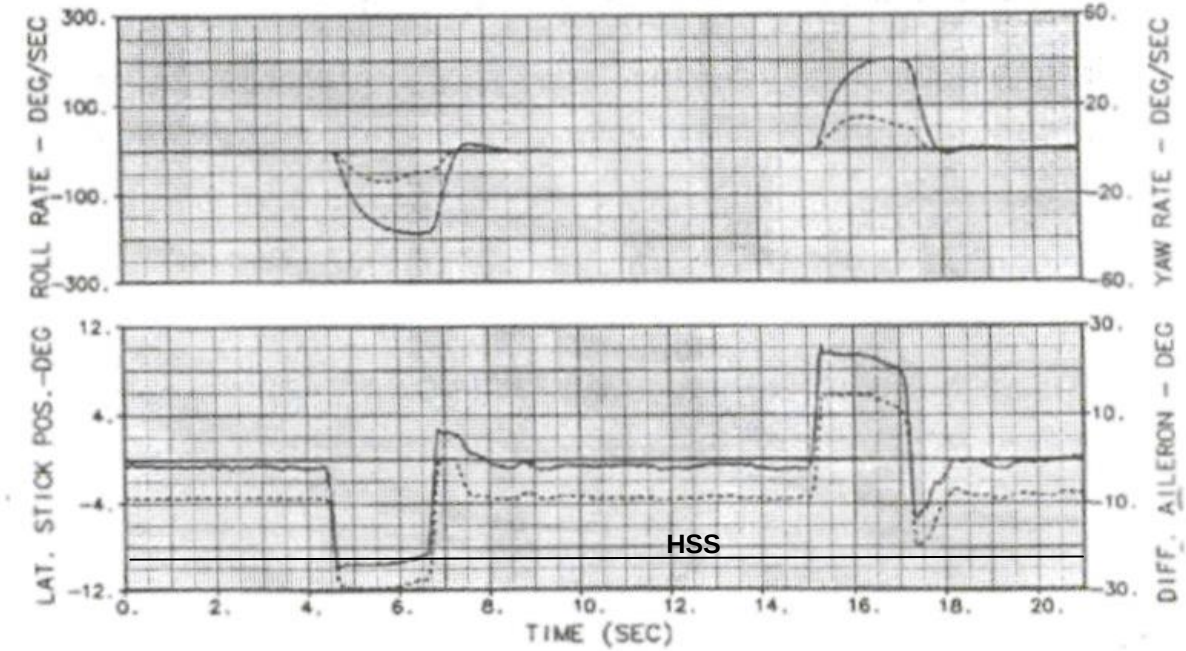

Figure 21. Example of flight data history of 360-degree roll maneuvers.

Figure 21 presents a left roll and a right roll maneuver. In the left roll, between four and eight, seconds, lateral stick in applied to slightly beyond the high-speed-stop (HSS) at 9 degrees and then is backed off slightly to just below the HSS. Aileron position remains fixed for a majority of the maneuver. During the right roll, the input is closer to the design, there is more back off. Looking at the roll rates that were achieved, the maximum roll rates occur when the lateral stick starts moving off the HSS. The original AFT applied lateral stick, to the design HSS of 9°, and held it through 360 degrees of roll. This resulted in a maximum roll rate 165°/s. When compared to the acceptance datum, 188°/s, there is a difference of 12.2%, which is out of the 10% acceptance tolerance. When the AFT is performed with a

more representative stick input, lateral stick to approximately 9.5°, the maximum roll rate increased to 176°/s, a difference of 6.3%, well within the acceptance tolerance.

Unfortunately situations such as the example above can be difficult to resolve if there are no flight data histories available. In those cases, educated assumptions pertaining to maneuver execution need to be made. In order to do this correctly, some investigation of alternative sources of data may be required. For example, an engineer could refer to test data from a similar aircraft and examine pilot input trends.

Evaluation Using Direct Simulation Overdrive (DSO)

In cases where no test was specified in the AFT for a particular maneuver, direct simulation overdrive was employed. This technique involved importing flight data or recreating flight data from reports and driving simulation input during a simulation run. Overdriving specific inputs allow the simulation to respond to precise conditions specified by flight or by a user. This technique allows engineers to drive an entire flight model by driving pilot input, or engineers can isolate a model by overdriving specific input to that model.

An application of this technique was the analysis of abrupt longitudinal inputs. Flight data were acquired from the US Navy for use in the development effort. These data contained aircraft state information as well as pilot input data and surface deflections.[20] For the analysis, the data were imported into the simulation and used to create overdrive signals for the AV-8B control surfaces. The simulation runs were executed by trimming to the desired aircraft state, then running the simulation in a batch mode. This technique allowed the engineers to examine the response of the six-degree-of-freedom simulation to flight measured input. Overdriving the control surfaces removed the control system from the simulation loop. Figure 22 contains diagram illustrating the overdrive loop with a sample comparison from the task.

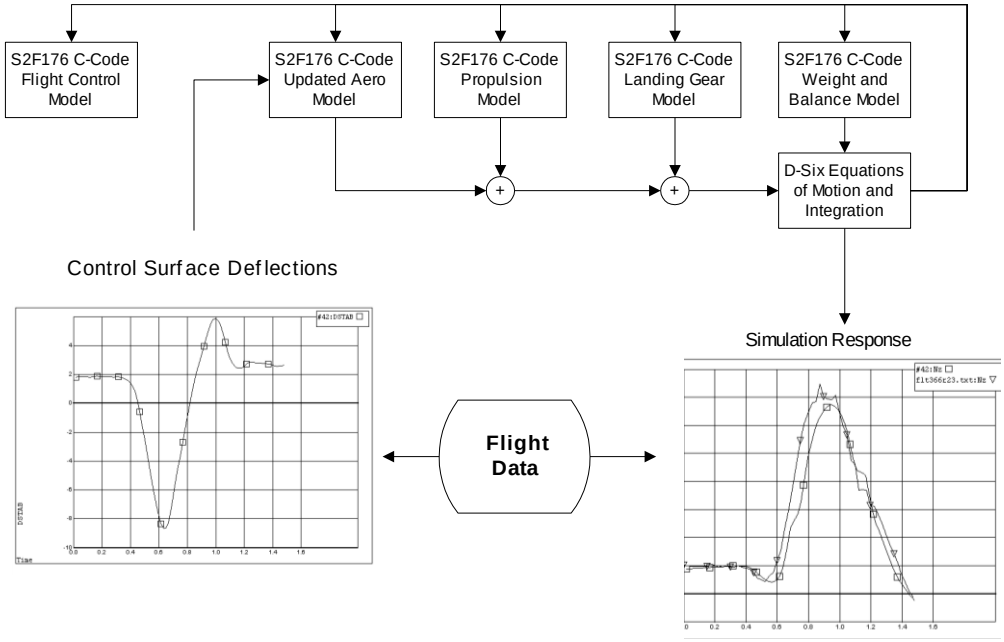

Figure 22. Diagram illustrating a partial simulation overdrive performed for the AV-8B and sample comparison plot.

Evaluation Using Desktop Piloted Simulation (DPS)

The desktop-piloted evaluations were performed using a commercial-off-the-shelf PC-Based simulation environment,[21] joystick, and throttle hardware. Other pilot inputs such as nozzle, gear, and flap position were provided by commands assigned by joystick and keyboard buttons. Flight information was provided to the pilot via head-up display (HUD) super imposed with an out-the-window (OTW) view of a flat terrain and engineering simulation variable display (ESVD). The HUD provided the pilot with a graphical indication of pitch, roll, heading, and flow angle changes, as well as altitude. It also provided

digital display of airspeed, Mach number, angle of attack, and bearing and range to a runway. The ESVD allowed the to display any variable used by the simulation. This display was particularly useful for displaying nozzle deflection, flap deflection, and surface deflections etc. Figure 23 contains a screen shot of the out-of-the-window display and HUD with the ESVD.

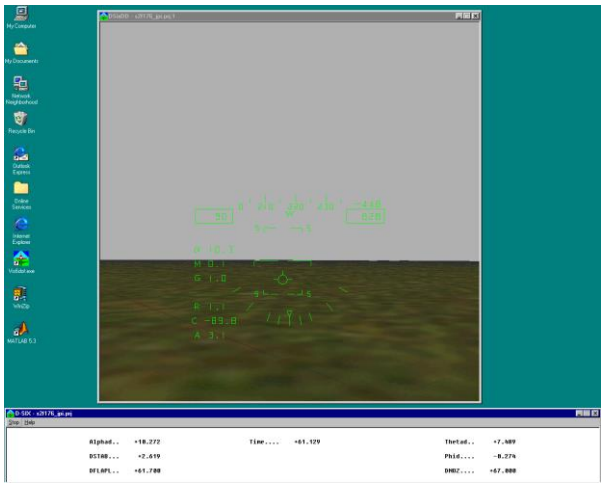

Figure 23. Screen capture during a desktop-piloted simulation session

Each piloted simulation session was run with the objective to execute maneuvers for which flight data were available in hard copy form only. This allowed BAR engineers to "fly" the simulation to aircraft states defined in histories of flight data and then execute maneuvers using the same technique used during flight tests. An example of this was in the evaluation of control power and lateral-directional characteristics at high angles of attack. The maneuvers in question were to be initiated in a wind-up turn to establish Mach number and desired angle of attack. Such maneuvers were difficult to execute using the AFT given limited resources, therefore they were performed using DPS.

At the start of each DPS the engineer would set all appropriate initial conditions including loading, flap setting, weight and center of gravity location, and aircraft state. The engineer would then start the simulation session employing the OTW graphics with HUD and execute the desired maneuver. Once completed satisfactorily, the data from the simulation run was either saved to disk or plotted for analysis and comparison with truth data. Figure 24 contains sample output from a vertical-takeoff and transition to wing-born flight.

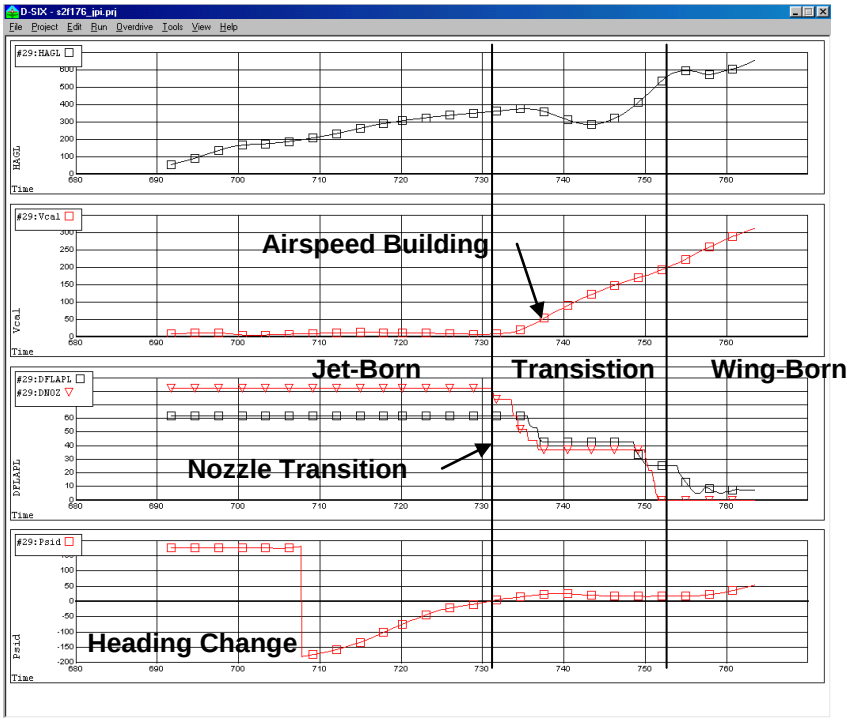

Figure 24. Simulation data from a DPS session performing a vertical take off and transition to wing born flight.

The ability to perform DPS and evaluate response of the flight model greatly reduced the amount of piloted time using trainer hardware.

As maneuvers were executed, simulation results were compared with flight data. If discrepancies were discovered, the area of the model was examined and solutions for model improvement were found and implemented. Using the available tools to in D-Six, very little time was required to modify the simulation model and run the simulation in real time. Therefore, engineers were able to perform model modifications and testing rapidly.

Evaluation Using Expert Pilot Evaluation (EPE)

The use of the pilot's inputs during the evaluation of the trainer model while operating the entire suite of trainer flight hardware is an important step in the validation of the model. The pilot has the ability to evaluate the general continuity of the model throughout the flight envelope as well as other aspects that are difficult or impossible to quantify by other evaluation techniques. Most simulation acceptance requirements place the pilot's response to the model as the final simulation acceptance criteria. Unfortunately for the engineer, this evaluation can be the most difficult of all to properly reconcile. When the pilot evaluates the flight model with the full trainer hardware in the loop, the flight model performance necessarily involves the other characteristics of the simulator hardware. One of the most significant external elements that can influence pilot evaluations is the characteristics of the controls, i.e. the control stick or control wheel. Because this provides the pilot with his primary feedback of the airplane response, improper modeling of control input behavior could have a significant effect on his impression of the flight behavior. Because the pilot's vision is also a primary sensory input during flight simulation, problems with the visual system can also result in the improper interpretation of flight model characteristics. In fixed based simulations, the lack of acceleration cues can also influence the pilot's interpretation of flight behavior in certain flight conditions.

In the development of the AV-8B flight model, as with any model development, the importance of the pilot's satisfaction with the model's response is paramount. This required close cooperation with the evaluation pilots in interpreting their comments, and as often as possible, extracting detailed descriptions of the desired behavior in quantitative terms. The development of the AV-8B model was eased somewhat through the participation of an experienced test pilot who was able to convey his comments in engineering terms. Further, his experience frequently allowed him to disconnect the flight model behavior from other portions of the trainer that also needed work, such as the control stick modeling. Nevertheless, other, less experienced pilots were also used in the evaluation of the flight model response, and careful interpretation of their comments was required.

The evaluation of the AV-8B trainer flight model rudder effectiveness is good example of the complexity of interpreting a pilot's comments pertaining to the flight-model fidelity. In this case, a an active duty pilot with over 1000 hours in the AV-8B was used to evaluate a number of the trainer's basic flight capabilities. After a series of maneuvers in the trainer, the pilot questioned the roll response to a rudder input. When the pilot applied left rudder pedal, the simulation produced a right-wing-down roll. In fact, the pilot claimed that this response was opposite to that exhibited in the real airplane. This comment led to a trainer deficiency report citing the behavior. Review of available flight records, along with more detailed evaluation of the simulation response using DPS, revealed that the response of the airplane to rudder inputs in roll was highly dependant on the trim angle of attack prior to and during the rudder input. This is because of the lack of lateral stability at low angles of attack not being able to counter the roll induced by the rudder deflection. Even though the rudder deflection results in a considerable sideslip excursion, the roll induced from the lateral stability is low at low angles of attack. Figure 25 contains data from a DPS session illustrating this effect. As the angle of attack increases, lateral stability increases as well, until above approximately 6° angle of attack, the roll due to sideslip is greater that that generated by the rudder deflection.

At this point, review of the piloted simulation sessions revealed that the pilot had performed all of the rudder rolls at angles of attack below 6°. Consequently, it was requested that he perform rudder rolls at a range of angles of attack in the airplane prior to his re-evaluation of the trainer. Following this, his review of the unchanged model revealed that the model was indeed correct, thus closing the discrepancy report.

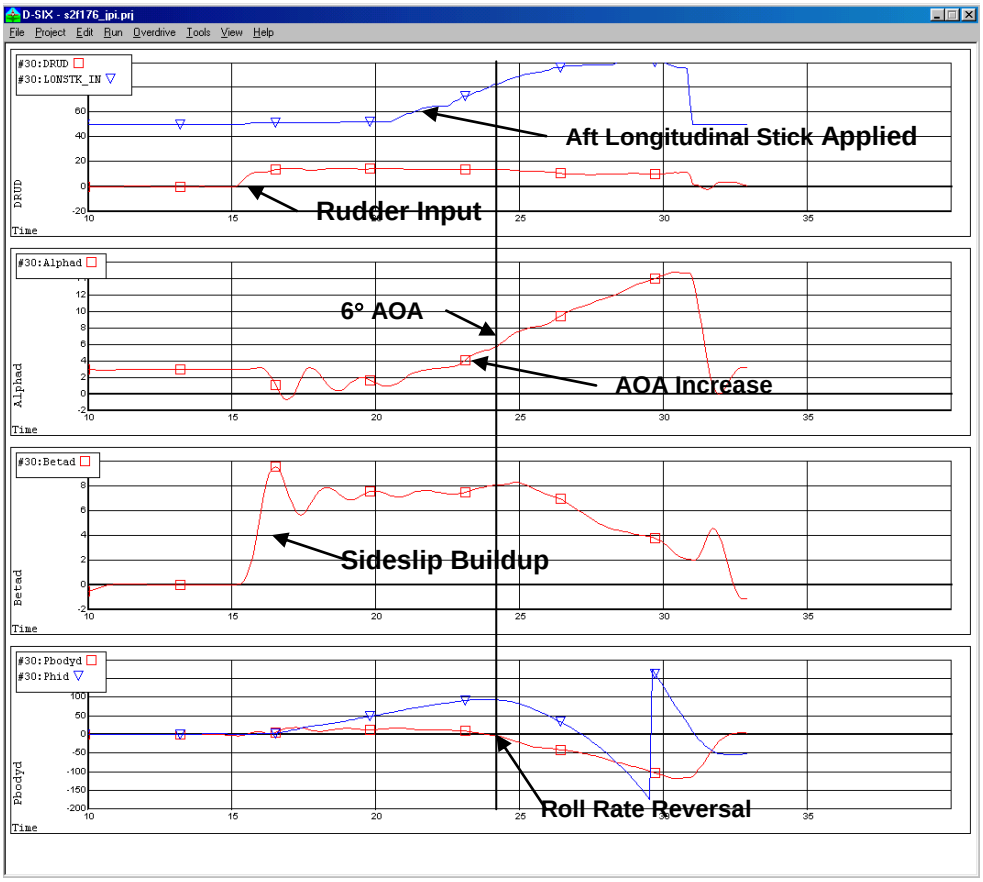

Figure 25. DPS data showing the effect of lateral-stability during a rudder input.

This example illustrates the difficulty in accurately interpreting pilot inputs and making model changes as a result. Without detailed review, the engineer could have easily modified the roll due to rudder or the lateral stability to provide the pilot with the perception of the correct behavior, but this response would have led to inaccuracies in other aircraft behaviors at other conditions. Whenever the model must be modified away from a known, documented data source, such as wind-tunnel results, flight results or other, it is highly desirable to have several pilots concur on the potential deficiency. Conversely, the simulation engineer should investigate all aspects of the reported deficiency.

Another example of piloted evaluation resulted in model changes. The AV-8B, while in the STOL, configuration, nozzle deflections greater than approximately 30 degrees and flaps also deflected greater than 25 degrees, exhibits a unique behavior in longitudinal flight characteristics when in ground effect. A nose-down pitching moment is caused by the reflection of jet blast on the ground with a resulting impingement on the aft portion of the aircraft, Figure 26. During takeoff, the pilot begins a ground roll with nozzles at 10 degrees. Once to the prescribed airspeed, based on weight, the nozzles are rotates to a prescribed angle, again based on loading and fuel. The rotation of the nozzles changes the thrust vector and lifts the aircraft from the ground. Shortly after lift off, the aircraft exhibits a nose-down pitch followed by a pitch-up once out of ground effect. The amount of pitching moment is a function of thrust setting, nozzle deflection, and aircraft center of gravity. Conversely, on short landing, as the aircraft approaches the ground the reflected blast impingement on the aircraft causes a nose-down moment. As a result, to perform a safe landing, the pilot is required to apply aft stick input that varies depending on aircraft center of gravity and power setting. Figure 27 contains a diagram illustrating this characteristic.[22]

As one would expect, the correct modeling of this situation is vitally important to student training. Unfortunately, during the early-piloted evaluations of the S2F176 trainer, the ground effect model was found to be deficient. Engineers then removed the old ground effect model and proceeded to construct a new ground effect.

The updated ground effect model was constructed in two parts, conventional and jet-reflection. The conventional portion of the ground effect model employed, as the name indicates, conventional ground effect modeling equations and were exercised then incorporated into the aerodynamics database as a function of height above ground. The second portion of the ground effect was more complex. Lacking test data, the model was structured to provide a physical representation of the jet blast reflection and impingement. The independent variables that effect the pitching moment of the aircraft were chosen to be gross thrust, height above terrain, and nozzle deflection. Airspeed also plays an effect, but was assumed to be negligible in the model. Assumptions were made pertaining to the jet-blast footprint and reflection thrust decay as height above terrain increased. These estimates were then used to determine a pitching moment coefficient based on the strength of the blast reflection and its impingement on the aircraft. The result was incorporated into the aerodynamics database as a function of gross thrust, nozzle deflection, and height above terrain.

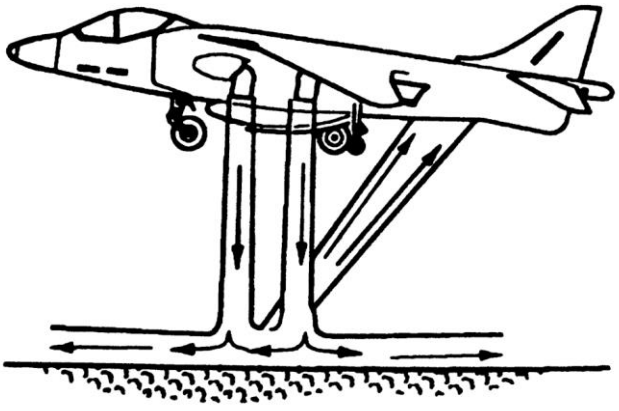

Figure 26. AV-8B NATOPS diagram illustrating jet blast reflection impingement with the aircraft

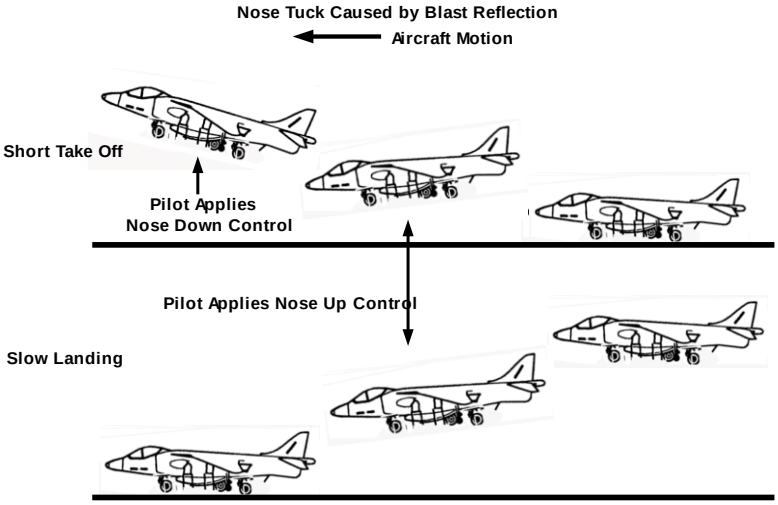

Figure 27. Diagram illustrating AV-8B motion due to jet blast reflection impingement with the aircraft during short take off and

This new ground effects model provided the trainer with a physically based model that is used for all modes of take off and landing. The model was implemented in the desktop simulation, tested, and evaluated. Engineers verified that the effect was in the model and operational. During the verification the effect was correlated with available trend information however, data in this flight regime were limited and engineers had no way of determining if the model provided the appropriate "feel" to the pilot. As a result, it was acknowledged that pilot-based "tuning" needed to be performed. The AV-8B pilots flew a series of short takeoffs and landings with a number of loadings and center of gravity locations and provided comments. Using pilot comments, engineers modified assumptions made during the development of the blast reflection ground effect modified the model. The newly updated model was retested using DPS and transmitted to the trainer for pilot revaluation. Figure 28, contains a comparison plot of two DPS hands-off short field takeoffs employing the new and old ground effect models. For each maneuver, the appropriate stabilator setting was used and pilot input consisted of only deflecting nozzles to 50 degrees. The plots reveal the effect of the increased nose-down pitching moment due to the blast reflection impingement. After several iterations, a physically based, representative ground effect model was incorporated as part of the trainer.

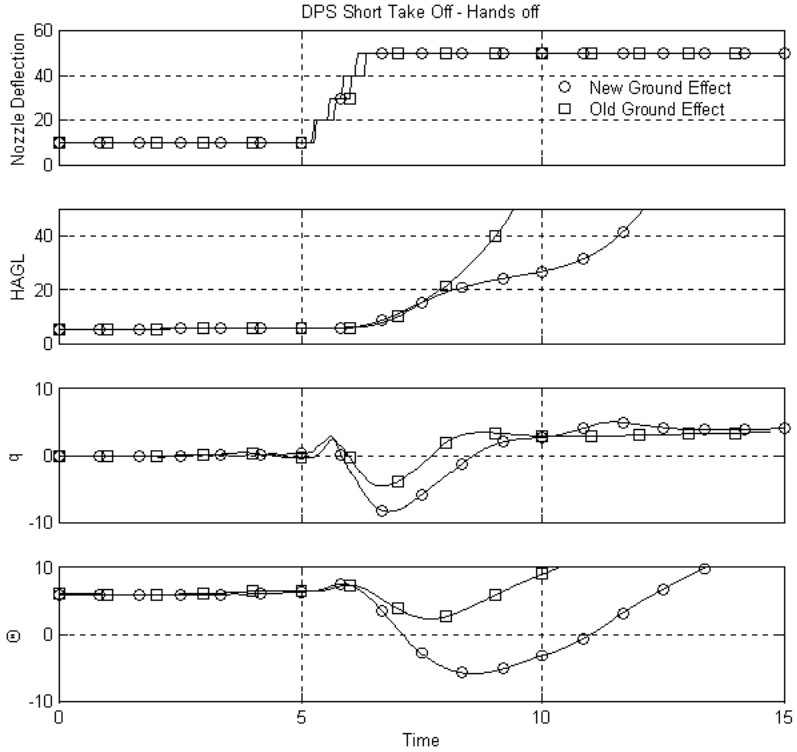

Figure 28. Hands off short take off using DPS employing new and old ground effect model

Summary

The evaluation and validation of the Italian Mission Simulator illustrates several important issues concerning both the engineer and pilot's role in the evaluation process. The use of an automated test tool for validation requires knowledge of not only the acceptance criteria, but also where it came from. The tool must be tuned to duplicate the appropriate maneuver input for comparison purposes. Otherwise, AFT results can be misleading and confusing, potentially leading to misapplied model corrections.

The use of techniques such a simulation overdrive provided a valuable tool to assess a model's response to a nonbiased aircraft input. This allows the engineer to focus on a specific model's fidelity rather than having to search for discrepancy sources.

This case also provides good examples of pilot feedback and how it can be a good source of information when it is accurate. Pilot awareness of aircraft state during a maneuver in the simulator and in the airplane is crucial when evaluation flight model behavior. As shown in the example rudder roll example, a little investigation prevented the inappropriate modification of the flight model. The second example of pilot feedback illustrated the process of a model modification resulting from the comments of several pilots. Gross modifications were postulated based on analytical means and then tested using DPS before pilot evaluation saving time and pilot resources. Once in the trainer the model was fine tuned with the feedback from *several* pilots. The word *several* is important. The use of multiple pilots during the tuning phase of the development helped improve model robustness.

REFERENCES

[1] *Webster's New World Dictionary of the American Language*, Warner Books, NY, 1987.

[2] Ralston, J.N. and Kay, J. "The Utilization of High Fidelity Simulation in the Support of High Angle of Attack Flight Testing." AIAA 96-XXX, August 1996.

[3] Nichols, J.H., "Controls Analysis and Simulation Test Loop Environment (CASTLE) User's Guide CASTLE Version 3.0," Naval Air Warfare Center Aircraft Division, Patuxent River, MD, 1993.

[4] Fitzgerald, T.R., et al, "Improvements to the Naval Air Warfare Center Aircraft Division's F/A-18 Subsonic Aerodynamics Model", AIAA-94-3400 Flight Simulation Technologies Conference in Scottsdale, AZ, 1-3 August 1994.

[5] Hess, Robert A., "Subsonic F/A-18A and F/A-18B (TF-18A) Aerodynamics Identified from Flight Test Data", SCT 4522-220-1, July 1987.

[6] Hess, Robert A., "Development and Evaluation of a High-Fidelity F-18 Aerodynamic Model in a Unified Format"; SCT 6007-070-1, October 1989.

[7] O'Connor, Cornelius, "NATC F-18A/B Aerodynamic Math Model Modifications Incorporated during the Phase II Model Unification Effort"; BAR 90-13, September 1990.

[8] "NATOPS Flight Manual: Navy Model F/A-18A/B/C/D"; A1-F18AC-NFM-000, 15 January 1991; change 5 — 15 August 1993.

[9] Bonner, M.S. and Gingras, D.R. "Status of a Comprehensive Validation of the Navy's F/A-18A/B/C/D Aerodynamics Model," AIAA-96-3529, 1996.

[10] Koehler, R. and Wilhelm, K., "Auslegung von Eingangssignalen für die Kennwertermittlung," IB 154-77/40, DFVLR Institut für Flugmechanik, Braunschweig, Federal Republic of Germany, December 1977.

[11] Klein, V., and Morgan, D., "Estimation of Bias Errors in Measured Airplane Responses Using Maximum Likelihood Method," NASA TM-89059, January 1987.

[12] Bonner, M. S., and Gingras, D. R., "Calibration of F/A-18 Power Approach Flight Data Collected with Production Sensors," paper to be published, 1997.

[13] Pindyck, R. S. and Rubinfield, D. L., Econometric Models and Economic Forecasts Third Edition, McGraw Hill, New York, NY, 1991.

[14] Klein, V., Batterson, J., and Murphy, P., "Determination of Airplane Model Structure From Flight Data by Using Modified Stepwise Regression," NASA TP-1916, October 1981.

[15] Klein, V., and Batterson, J., "Determination of Airplane Model Structure From Flight Data Using Splines and Stepwise Regression," NASA TP-2126, March 1983.

[16] Balderson, K.A., Gaublomme, D.P., and Thomas, J.W., "Simulation Validation Through Linear Model Comparison," AIAA-96-3530-CP, July 1996

[17] Coleman, H.W., and Steele, W.G., Experimentation and Uncertainty Analysis for Engineers, John Wiley & Sons, New York, NY, 1989.

[18] Gingras, D.R. “AV-8B II+ Device S2F176 Flight Model Development Using A PC-Based Simulation Environment”, AIAA-4191, August 1999.

[19] McDonnell Douglas Aircraft Corporation. "Aircraft Stability and Control and Flying Qualities, Supplement VI - Radar Integration Flight Test Results," MDC A5192 Supplement VI Rev A, November 1995.

[20] McDonnell Douglas Aircraft Corporation. Aircraft Stability and Control and Flying Qualities, Supplement IV - 100% LERX Flight Test Results, Vol I-IV, MDC A5192, March 1992.

[21] Bell, J.W. and O’Rourke, M.J. Application of a Multipurpose Simulation Design, AIAA 97-3798.

[22] United States Navy NATOPS Flight Manual for the AV-8B/TAV-8B.